

PRECONDITIONING OF WEIGHTED $H(\text{div})$ -NORM AND APPLICATIONS TO NUMERICAL SIMULATION OF HIGHLY HETEROGENEOUS MEDIA

JOHANNES KRAUS, RAYTCHO LAZAROV, MARIA LYMBERY, SVETOZAR MARGENOV, AND LUDMIL ZIKATANOV

ABSTRACT. In this paper we propose and analyze a preconditioner for a system arising from a finite element approximation of second order elliptic problems describing processes in highly heterogeneous media. Our approach uses the technique of multilevel methods (see, e.g. [16]) and the recently proposed preconditioner based on additive Schur complement approximation by J. Kraus (see, [8]). The main results are the design and a theoretical and numerical justification of an iterative method for such problems that is robust with respect to the contrast of the media, defined as the ratio between the maximum and minimum values of the coefficient (related to the permeability/conductivity).

1. INTRODUCTION

We consider the following second order elliptic boundary value problem written in mixed form for the unknown scalar functions $p(x)$ and the vector function \mathbf{u} :

$$\begin{aligned} (1.1a) \quad & \mathbf{u} + K(x)\nabla p = 0 \quad \text{in } \Omega, \\ (1.1b) \quad & \text{div } \mathbf{u} = f \quad \text{in } \Omega, \\ (1.1c) \quad & p = 0 \quad \text{on } \Gamma_D, \\ (1.1d) \quad & \mathbf{u} \cdot \mathbf{n} = 0 \quad \text{on } \Gamma_N. \end{aligned}$$

Here, $K : \mathbb{R}^d \mapsto \mathbb{R}^{d \times d}$ is a function taking values in symmetric, positive definite (SPD) $d \times d$ matrices for almost all $x \in \Omega$. The given forcing term f is function in $L^2(\Omega)$, $\Omega \subset \mathbb{R}^d$ ($d = 2, 3$) is a bounded polyhedral domain, and its boundary $\partial\Omega$ is split into two non-overlapping parts Γ_D and Γ_N . In the case pure Neumann problem, i.e. $\Gamma_N = \partial\Omega$, we assume that f satisfies the compatibility condition $\int_{\Omega} f dx = 0$. In such a case the solution is determined uniquely by taking $\int_{\Omega} p dx = 0$. To simplify our presentation, we shall assume that Γ_D is an non-empty set with strictly positive measure which is also closed with respect to $\partial\Omega$, so the above problem has unique solution $p \in H^1(\Omega)$.

This equation is a model used for example in heat and mass transfer, flows in porous media, diffusion of passive chemicals, electromagnetics, and other applied areas. Here we target applications of equations (1.1a) - (1.1d) to flows in *highly heterogeneous* media of high contrast. This means that the coefficient $K(x)$ represents media with multiscale features, such as many inclusions where $K(x)$ has small values and long connected subdomains where $K(x)$ has large values. An important characteristic for such media is the contrast κ , defined by (2.1). In the terminology of flows in porous media the coefficient $K(x)$ is called permeability and the unknown variables p and \mathbf{u} are called pressure and velocity, respectively.

Flows in porous media appear in many industrial, scientific, engineering, and environmental applications. One common characteristic of these diverse areas of applications is that porous media are intrinsically multiscale and typically display heterogeneities over a wide range of length-scales.

Date: February 26, 2013–beginning; Today is February 6, 2024.

1991 Mathematics Subject Classification. 65F10, 65N20, 65N30.

Key words and phrases. mixed finite elements, least-squares, high contrast media, robust preconditioners for weighted $\mathbf{H}(\text{div})$ -norm, discrete Poincaré inequality.

The computer generated permeability coefficient $K(x)$ which exhibits such features and is used in petroleum engineering simulations as a benchmark is found in the SPE10 Project [7].

Depending on the application and its goals, solving the governing equations of flows in porous media might be sought at: (a) a coarse scale (e.g., if only the global pressure drop for a given flow rate is needed, and no other fine scale details of the solution are important), or a coarse scale enriched with some desirable fine scale details, and (b) the finest scale that resolves media heterogeneities, if computationally this is possible. The numerical solution of latter class of problems is a challenging task that has attracted a substantial attention in the scientific and engineering community.

The aim of this paper is finite element approximations of the problem (1.1a) – (1.1d) on a mesh that resolves the finest scale of the permeability. This leads to a very large system of algebraic equations and its efficient solution is the object of this paper. We give two finite element approximations, dual mixed and least-squares FEM, and develop, study and test an optimal (with respect to the contrast κ and the mesh size h) preconditioner for the corresponding algebraic problem.

The system arising from the finite element approximation has symmetric matrix, which is indefinite in the case of a mixed method and positive definite in the case of a least-squares approximation. In both cases the preconditioner is a block diagonal matrix, which in combination with a minimal residual method in the case of mixed method and conjugate gradient iteration in the case of least-squares FEM, leads to an optimal preconditioner so that the number of iterations does not depend neither on the contrast nor on the mesh size.

In the least-squares methods written as a system of linear equations for the unknown \mathbf{u} and p , the upper left block (corresponding to the vector variable \mathbf{u}) is a symmetric and positive definite matrix, corresponding to the finite element approximation of the weighted bilinear form $(K^{-1}\mathbf{u}, \mathbf{v}) + (\operatorname{div} \mathbf{u}, \operatorname{div} \mathbf{v})$ with $\mathbf{H}(\operatorname{div})$ -conforming finite elements. For the mixed method this form plays also essential role (see, e.g. [1]). It is known that the preconditioner of Arnold, Falk, and Winther, [1, 2], is optimal if $K(x)$ is a constant matrix. However, since $K(x)$ is the permeability of heterogeneous media of high contrast, the corresponding matrix is very ill-conditioned and consequently construction of an optimal preconditioner is a nontrivial task. The main result and novelty of this paper is design, theoretical justification, and experimental study of a preconditioner for the matrix corresponding to the above weighted bilinear form that will produce an optimal iterative method which converges independently of the contrast κ . Such construction is based on the method developed in [9].

The paper is organized as follows. In Section 2 the dual mixed and least-squares variational formulations of the boundary value problem (1.1a)–(1.1d) are given. Next we introduce the weighted $\mathbf{H}(\operatorname{div})$ bilinear form and show proper inf-sup condition using the corresponding weighted norm. We emphasize that the constant in the inf-sup condition, coercivity and the boundedness of the corresponding forms do not depend on the contrast of the media defined by (2.1). In Section 3 we introduce finite element approximations for the mixed and least-squared formulations. A key point in this part is Lemma 3.1 where we establish an inf-sup condition on a discrete level with a constant independent on the contrast. The detailed proof of the Lemma is given in the Appendix. In Section 4, which is central to the paper, we describe the preconditioning method for the finite element systems. Starting with the definition of a block-diagonal preconditioner for the dual-mixed formulation in operator notation, see Section 4.1, a reformulation of the FE problem in matrix notation is given in Section 4.2. The key issue in designing a contrast-independent Krylov solver becomes the construction of a robust preconditioner for the weighted $H(\operatorname{div})$ -norm. This is addressed in details in Section 4.3 by, first, discussing an abstract auxiliary space two-grid method, see Section 4.3.1, and then, defining an auxiliary space multigrid (ASMG) method, see Section 4.3.2. Two variants of the algorithm are described in Section 4.3.3 differing only in the choice of the basis in which smoothing and residual updates are performed. Finally, in Section 5, we present the numerical results for three different examples of porous media in two dimensions in order to test

the robustness of the preconditioner with respect to media contrast and its optimality with respect to the mesh-size. All numerical results confirm our theoretical findings.

2. PROBLEM FORMULATION

2.1. Notation and preliminaries. For functions defined on Ω we shall use the standard notations for Sobolev spaces. Namely, $H^s(\Omega)$, $s \geq 0$ an integer, is the space of functions having their generalized derivatives up to order s square-integrable on Ω . We denote by (\cdot, \cdot) the L^2 and $[L^2]^d$ inner products. The standard norms on H^s are denoted by $\|\cdot\|_s$. For $s = 0$ we shall often use $\|\cdot\|$ without subscript. When the norm is weighted with a matrix valued function $\omega(x)$, with $\omega(x)$ SPD for almost all $x \in \Omega$ we use the notation:

$$\|\mathbf{v}\|_{0,\omega} := \|\omega^{1/2}\mathbf{v}\|, \quad |\phi|_{1,\omega} := \|\nabla\phi\|_{0,\omega} = \|\omega^{1/2}\nabla\phi\|.$$

Occasionally, when we consider only a subset of Ω , say, $T \subset \Omega$ we will indicate this in the notation for the norms and seminorms, i.e., we have $\|\cdot\|_{s,T}$, $\|\cdot\|_{s,\omega,T}$, $|\cdot|_{s,T}$, and $|\cdot|_{s,\omega,T}$.

In the following, if $\omega \in \mathbb{R}^{d \times d}$ is symmetric matrix, the norm $\|\omega\|_{\ell^2}$ is, as usual, the spectral radius of ω . We introduce the number

$$(2.1) \quad \kappa = \max_{x \in \Omega} (\|K(x)\|_{\ell^2} \|K^{-1}(x)\|_{\ell^2}).$$

called the contrast of the media, is assumed that this could be many orders of magnitude. For scalar permeability $K(x)$, obviously, $\kappa = \max_{x \in \Omega} K(x) / \min_{x \in \Omega} K(x)$. The values of κ typically are very large (up to 10^8).

The Hilbert space $\mathbf{H}(\text{div})$ consists of square-integrable vector-fields on Ω with square-integrable divergence. The inner product in $\mathbf{H}(\text{div})$ is given by

$$(2.2) \quad \Lambda(\mathbf{u}, \mathbf{v}) = (\mathbf{u}, \mathbf{v}) + (\text{div } \mathbf{u}, \text{div } \mathbf{v}).$$

Further we use the notation of the Sobolev spaces $H_D^1(\Omega)$ and $\mathbf{H}_N(\text{div})$

$$(2.3) \quad H_D^1(\Omega) = \{\phi \in H^1(\Omega) : \phi(x) = 0 \text{ on } \Gamma_D\}.$$

In the case when $\Gamma_D = \emptyset$ we have

$$(2.4) \quad H_D^1(\Omega) = \{\phi \in H^1(\Omega) : \int_{\Omega} \phi = 0\}.$$

Note that for $\phi \in H_D^1(\Omega)$ the seminorms $|\phi|_1 = \|\nabla\phi\|$ and $|\phi|_{1,\omega} = \|\omega^{1/2}\nabla\phi\|$ are in fact norms on $H_D^1(\Omega)$ and we denote these norms by $\|\phi\|_1$ and $\|\phi\|_{1,\omega}$. The space $\mathbf{H}_N(\text{div})$ is defined as follows:

$$(2.5) \quad \mathbf{H}_N(\text{div}) := \mathbf{H}_N(\text{div}; \Omega) = \{\mathbf{v} \in \mathbf{H}(\text{div}; \Omega) : \mathbf{v}(x) \cdot \mathbf{n} = 0 \text{ on } \Gamma_N\}.$$

Together with (2.2) the weighted inner product in the space $\mathbf{H}(\text{div})$ will play a fundamental role in our analysis

$$(2.6) \quad \Lambda_{\alpha}(\mathbf{u}, \mathbf{v}) = (\alpha \mathbf{u}, \mathbf{v}) + (\text{div } \mathbf{u}, \text{div } \mathbf{v}), \quad \alpha(x) = K^{-1}(x).$$

We also denote

$$\|\mathbf{v}\|_{\Lambda_{\alpha}}^2 = \Lambda_{\alpha}(\mathbf{v}, \mathbf{v}) = \|\mathbf{v}\|_{0,\alpha}^2 + \|\text{div } \mathbf{v}\|^2.$$

Note, that a weighted bilinear form of the type $\Lambda_{\alpha,\beta}(\mathbf{u}, \mathbf{v}) = \alpha(\mathbf{u}, \mathbf{v}) + \beta(\text{div } \mathbf{u}, \text{div } \mathbf{v})$, with $\alpha > 0$ and $\beta > 0$ constants, was used by Arnold, Falk, and Winther in [2] to design multigrid methods for $\mathbf{H}(\text{div})$ -systems. A key moment in their study was the construction of a multigrid method that converges uniformly with respect to the parameters α and β . The important difference between our bilinear form Λ_{α} compared with $\Lambda_{\alpha,\beta}$ is that in our form α is a highly heterogeneous function with high contrast. This makes the proof of a proper *inf-sup* condition more delicate and the construction of an efficient preconditioner more complicated.

The main objective of this work is a derivation and theoretical justification of numerical methods for solving the problem (1.1a) – (1.1d) that are robust with respect to the media contrast, or in

the ideal case, do not depend on the contrast κ . In this regard, in the following we write $x \lesssim y$ to denote the existence of a constant C such that $x \leq Cy$. In case $x \lesssim y$ and $y \lesssim x$ we write $x \approx y$. It is important to remember that in our analysis the constants hidden in \lesssim or \approx are always independent of the contrast and the mesh size.

Note that for all $\xi \in \mathbb{R}^d$, $x \in \Omega$ and writing K for $K(x)$ we have

$$\begin{aligned} \|K^{-1}\|_{\ell^2(K\xi \cdot \xi)} &\geq (\xi \cdot \xi) \|K^{-1}\|_{\ell^2} \inf_{\theta \in \mathbb{R}^d} \frac{(K\theta \cdot \theta)}{(\theta \cdot \theta)} \\ &= (\xi \cdot \xi) \|K^{-1}\|_{\ell^2} \inf_{\theta \in \mathbb{R}^d} \frac{(\theta \cdot \theta)}{(K^{-1}\theta \cdot \theta)} = (\xi \cdot \xi) \|K^{-1}\|_{\ell^2} \frac{1}{\|K^{-1}\|_{\ell^2}} = (\xi \cdot \xi). \end{aligned}$$

Based on this, without loss of generality we assume that the following inequality holds

$$(2.7) \quad (\xi \cdot \xi) \leq (K(x)\xi \cdot \xi), \quad \xi \in \mathbb{R}^d.$$

As seen from the considerations above, such an assumption is always fulfilled if we scale the coefficient and work with

$$K(x) \leftarrow K(x) \left\| \|K^{-1}(x)\|_{\ell^2} \right\|_{L^\infty(\Omega)}.$$

Clearly, such rescaling does not change the value of κ .

We note that the standard elliptic theory ensures existence and uniqueness of a unique solution $p \in H_D^1(\Omega)$. However, since the coefficient matrix $K(x)$ is piece-wise smooth and may have very large jumps, the solution p has low regularity, say $H^{1+s}(\Omega)$, where $s > 0$ could depend on the contrast κ in a subtle (and unfavorable) way. We need to take this into account when proving the stability of the discrete methods with constants independent of κ .

2.2. Weak formulations of the elliptic problem. Now we introduce the dual mixed and least-squares formulations of the problem (1.1a) – (1.1d).

2.2.1. Dual mixed formulation. To present the dual mixed weak form we require the following notation $\mathbf{V} \equiv \mathbf{H}_N(\text{div}; \Omega)$ and $W \equiv \{q \in L^2(\Omega) \text{ and } (q, 1) = 0 \text{ if } \Gamma_N = \partial\Omega\}$.

We multiply the first equation by $K^{-1}(x)$ and a test function \mathbf{v} , integrate over Ω , and perform integration by parts to get

$$(2.8) \quad (K^{-1}(x)\mathbf{u}, \mathbf{v}) - (p, \text{div } \mathbf{v}) = 0$$

Next, we multiply the second equation by a test function q and integrate over Ω to get

$$(2.9) \quad (\text{div } \mathbf{u}, q) = (f, q).$$

Then the weak form of the problem (1.1a) – (1.1d) is: find $\mathbf{u} \in \mathbf{V}$ and $p \in W$ such that

$$(2.10) \quad \mathcal{A}^{DM}(\mathbf{u}, p; \mathbf{v}, q) = -(f, q), \quad \text{for all } (\mathbf{v}, q) \in \mathbf{V} \times W,$$

where the bilinear form $\mathcal{A}^{DM}(\mathbf{u}, p; \mathbf{v}, q) : (\mathbf{V}, W) \times (\mathbf{V}, W) \rightarrow \mathbb{R}$ is defined as

$$(2.11) \quad \mathcal{A}^{DM}(\mathbf{u}, p; \mathbf{v}, q) := (\alpha \mathbf{u}, \mathbf{v}) - (p, \text{div } \mathbf{v}) - (\text{div } \mathbf{u}, q).$$

Remark 2.1. It is clear that we could test the equation (2.9) with $q = \text{div } \mathbf{v}$, multiply by an arbitrary positive constant β , and add to equation (2.8). This will result in a slightly different bilinear form

$$\mathcal{A}_\beta^{DM}(\mathbf{u}, p; \mathbf{v}, q) := (\alpha \mathbf{u}, \mathbf{v}) + \beta(\text{div } \mathbf{u}, \text{div } \mathbf{v}) - (p, \text{div } \mathbf{v}) - (\text{div } \mathbf{u}, q).$$

and modified right hand side of (2.10) equal to $-(f, q) + \beta(f, \text{div } \mathbf{v})$. This modified problem will have the same solution. However, such formulation might be beneficial in the design of a better preconditioner for the finite element system, see, e.g. [17].

2.2.2. Least-squares formulation. In this case we take the L^2 -norm of the second equation (1.1b) and the weighted L^2 -norm with weight $K^{-1/2}$ of the first equations in (1.1a) to obtain a quadratic functional, e.g. [15]. Then the minimizer of this least-squares functional satisfies the following weak form: find $\mathbf{u} \in \mathbf{H}_N(\text{div})$ and $p \in H_D^1(\Omega)$ such that

$$(2.12) \quad \mathcal{A}^{LS}(\mathbf{u}, p; \mathbf{v}, q) = (f, \text{div } \mathbf{v}), \quad \text{for all } (\mathbf{v}, q) \in \mathbf{H}_N(\text{div}) \times H_D^1(\Omega),$$

where the bilinear form $\mathcal{A}^{LS}(\mathbf{u}, p; \mathbf{v}, q) : (\mathbf{H}_N(\text{div}), H_D^1(\Omega)) \times (\mathbf{H}_N(\text{div}), H_D^1(\Omega)) \rightarrow \mathbb{R}$ is defined as

$$(2.13) \quad \mathcal{A}^{LS}(\mathbf{u}, p; \mathbf{v}, q) := (\alpha \mathbf{u}, \mathbf{v}) + (\text{div } \mathbf{u}, \text{div } \mathbf{v}) + (p, \text{div } \mathbf{v}) + (\text{div } \mathbf{u}, q) + (K \nabla p, \nabla q).$$

Clearly, the bilinear form $\mathcal{A}^{LS}(\mathbf{u}, p; \mathbf{v}, q)$ is symmetric and coercive, see, e.g. [15]. We would like to establish the coercivity with a constant independent of the contrast κ and later we provide a proof of this.

2.3. Stability of the weak formulations. Now we study the stability of the discrete problems (2.10) and (2.12). We shall use the Poincaré inequality

$$(2.14) \quad \text{there is } C_P > 0 \text{ such that for all } q \in H_D^1(\Omega) \quad \|q\|^2 \leq C_P \|\nabla q\|^2.$$

The constant C_P depends only on the geometry of the domain Ω and the splitting of $\partial\Omega$ into Γ_D and Γ_N . Moreover, due to (2.7) on the coefficient $K(x)$ we also have the inequality

$$\|q\|^2 \leq C_P \|\nabla q\|^2 \leq C_P \|\nabla q\|_{0,K}^2.$$

2.3.1. Stability of the mixed formulation. First, we consider the mixed form. For this we need continuity and *inf-sup* condition (see, e.g. [5]) for the bilinear form $\mathcal{A}^{DM}(\mathbf{u}, p; \mathbf{v}, q)$ on the spaces \mathbf{V} and $L^2(\Omega)$ equipped with the weighted norm $(\Lambda_\alpha(\mathbf{v}, \mathbf{v}))^{1/2}$ and the standard L^2 -norm $\|p\|$, respectively.

Lemma 2.1. *Let $W = L^2(\Omega)$, $\mathbf{V} = \mathbf{H}_N(\text{div})$, and $\|\mathbf{v}\|_{\Lambda_\alpha} := (\Lambda_\alpha(\mathbf{v}, \mathbf{v}))^{1/2}$. Then the following inequalities hold*

(1) *For all $\mathbf{u}, \mathbf{v} \in \mathbf{V}$ and for all $p, q \in W$*

$$(2.15) \quad \mathcal{A}^{DM}(\mathbf{u}, p; \mathbf{v}, q) \leq (\|\mathbf{u}\|_{\Lambda_\alpha}^2 + \|p\|^2)^{1/2} (\|\mathbf{v}\|_{\Lambda_\alpha}^2 + \|q\|^2)^{1/2};$$

(2) *There is a constant $\alpha_0 > 0$ independent of α such that*

$$(2.16) \quad \sup_{\mathbf{v} \in \mathbf{V}, q \in L^2} \frac{\mathcal{A}^{DM}(\mathbf{u}, p; \mathbf{v}, q)}{(\|\mathbf{v}\|_{\Lambda_\alpha}^2 + \|q\|^2)^{1/2}} \geq \alpha_0 (\|\mathbf{u}\|_{\Lambda_\alpha}^2 + \|p\|^2)^{1/2}$$

Proof. The first inequality follows immediately by applying Schwarz inequality to all three terms and having in mind that α is a positive function. Proving the *inf-sup* condition (2.16) is equivalent to proving the following inequality (see, [6]):

$$(2.17) \quad \inf_{q \in W} \sup_{\mathbf{v} \in \mathbf{V}} \frac{(\nabla \cdot \mathbf{v}, q)}{\|\mathbf{v}\|_{\Lambda_\alpha} \|q\|} \geq \gamma > 0, \quad \text{for all } \mathbf{v} \in \mathbf{V}, \quad \text{for all } q \in W.$$

As is well known, if γ is independent of the contrast κ , then so is α_0 and for more details on the relation between the constants γ and α_0 we refer to [19]. It is clear then that proving a contrast independent estimate for γ , which we show next, automatically leads to a contrast independent α_0 .

Inf-sup condition (2.17) for Raviart-Thomas finite element spaces and standard $\mathbf{H}_N(\text{div})$ -norm is a well known fact. However, we have slight modification the $\mathbf{H}_N(\text{div})$ -norm and we would like to show that the constant γ does not depend on the contrast κ . For this reason we provide a proof.

We first prove that for all $q \in W$ there exists $\mathbf{w} \in \mathbf{V}$ such that

$$(2.18) \quad \|\mathbf{w}\|_{0,\alpha}^2 \leq C_P \|q\|^2.$$

For this let $\varphi \in H_D^1(\Omega)$ be the solution to the variational problem

$$(2.19) \quad (K(x) \nabla \varphi, \nabla \chi) = (q, \chi), \quad \text{for all } \chi \in H_D^1(\Omega).$$

We then set $\mathbf{w} = K\nabla\varphi$. By construction $\mathbf{w} \in \mathbf{V}$ with $\operatorname{div} \mathbf{w} = -q$ which holds in $L^2(\Omega)$. Since $\alpha K = I_{d \times d}$ for almost all $x \in \Omega$, then

$$\begin{aligned} \|\mathbf{w}\|_{0,\alpha}^2 &= (\alpha K\nabla\varphi, \mathbf{w}) = (\nabla\varphi, \mathbf{w}) = -(\varphi, \operatorname{div} \mathbf{w}) = (\varphi, q) \\ &\leq \|\varphi\| \|q\| \leq \sqrt{C_P}(\nabla\varphi, \nabla\varphi)^{\frac{1}{2}} \|q\| \\ &\leq \sqrt{C_P} |\nabla\varphi|_{0,K} \|q\| = \sqrt{C_P} \|\mathbf{w}\|_{0,\alpha} \|q\|. \end{aligned}$$

Here, we used the Poincaré inequality (2.14) and the fact that from (2.7) we have $(K(x)\xi \cdot \xi) \geq (\xi \cdot \xi)$ for $\xi \in \mathbb{R}^d$ and $x \in \Omega$.

Next, for any $q \in L^2(\Omega)$ we have

$$\begin{aligned} \sup_{\mathbf{v} \in \mathbf{V}} \frac{(q, \operatorname{div} \mathbf{v})}{\|\mathbf{v}\|_{\Lambda_\alpha}} &\geq \frac{(q, \operatorname{div} \mathbf{w})}{\|\mathbf{w}\|_{\Lambda_\alpha}} = \frac{\|q\|^2}{(\|\mathbf{w}\|_{0,\alpha}^2 + \|\operatorname{div} \mathbf{w}\|^2)^{\frac{1}{2}}} \\ &= \frac{\|q\|^2}{(\|\mathbf{w}\|_{0,\alpha}^2 + \|q\|^2)^{\frac{1}{2}}} \geq \frac{\|q\|}{\sqrt{C_P + 1}}. \end{aligned}$$

This completes the proof. \square

2.3.2. Stability of the least-squares formulation. For this we require continuity and coercivity of the bilinear form $\mathcal{A}^{LS}(\mathbf{u}, p; \mathbf{v}, q)$ on the space $\mathbf{H}_N(\operatorname{div}) \times H_0^1(\Omega) \equiv \mathbf{V} \times W$. The space $\mathbf{H}_N(\operatorname{div})$ is equipped with the weighted norm $(\Lambda_\alpha(\mathbf{v}, \mathbf{v}))^{\frac{1}{2}}$ and the space $H_D^1(\Omega)$ is equipped with the norm $\|q\|_{1,K} = \|K^{1/2}\nabla q\|$.

Lemma 2.2. *Let $W = H_D^1(\Omega)$ and $\mathbf{V} = \mathbf{H}_N(\operatorname{div})$. Then the following inequalities hold:*

(1) *For all $\mathbf{u}, \mathbf{v} \in \mathbf{V}$ and for all $p, q \in W$*

$$(2.20) \quad \mathcal{A}^{LS}(\mathbf{u}, p; \mathbf{v}, q) \leq 2(\|\mathbf{u}\|_{\Lambda_\alpha}^2 + \|p\|_{1,K}^2)^{\frac{1}{2}}(\|\mathbf{v}\|_{\Lambda_\alpha}^2 + \|q\|_{1,K}^2)^{\frac{1}{2}};$$

(2) *For all $\mathbf{v} \in \mathbf{V}$ and $q \in W$ then*

$$(2.21) \quad \mathcal{A}^{LS}(\mathbf{v}, q; \mathbf{v}, q) \geq \frac{1}{3}(\|\mathbf{v}\|_{\Lambda_\alpha}^2 + \|q\|_{1,K}^2)$$

Proof. The bound (2.20) follows easily by first transforming the terms $(\operatorname{div} \mathbf{u}, q)$ and $(\operatorname{div} \mathbf{v}, p)$ using integration by parts to $-(\nabla q, \mathbf{u})$ and $-(\nabla p, \mathbf{v})$ and then using Schwarz inequality.

For the bound (2.21) we first note that

$$(2.22) \quad \mathcal{A}^{LS}(\mathbf{v}, q; \mathbf{v}, q) = \|\operatorname{div} \mathbf{v}\|^2 + (\alpha \mathbf{v} - \nabla q, \mathbf{v} - K\nabla q) \geq \|\operatorname{div} \mathbf{v}\|^2.$$

Next, we proceed as follows: using the Schwarz inequality, the Poincaré inequality, $\alpha K = I_{d \times d}$, and also $2ab \leq \frac{1}{\epsilon}a^2 + \epsilon b^2$ for all $\epsilon > 0$, $a, b \in \mathbb{R}$ gives

$$\begin{aligned} \mathcal{A}^{LS}(\mathbf{v}, q; \mathbf{v}, q) &\geq (1 - \frac{1}{\epsilon})\|\operatorname{div} \mathbf{v}\|^2 + \|\mathbf{v}\|_{0,\alpha}^2 + \|q\|_{1,K}^2 - \epsilon\|q\|^2 \\ &\geq (1 - \frac{1}{\epsilon})\|\operatorname{div} \mathbf{v}\|^2 + \|\mathbf{v}\|_{0,\alpha}^2 + (1 - \epsilon C_P)\|\nabla q\|_{0,K}^2, \quad \epsilon > 0. \end{aligned}$$

Choosing $\epsilon = \frac{1}{2C_P}$ we get

$$\mathcal{A}^{LS}(\mathbf{v}, q; \mathbf{v}, q) \geq (1 - 2C_P)\|\operatorname{div} \mathbf{v}\|^2 + \|\mathbf{v}\|_{0,\alpha}^2 + \frac{1}{2}\|\nabla q\|_{0,K}^2.$$

Now multiplying inequality (2.22) by a constant $\beta > 0$ and adding it to this inequality we have

$$(1 + \beta)\mathcal{A}^{LS}(\mathbf{v}, q; \mathbf{v}, q) \geq (1 - 2C_P + \beta)\|\operatorname{div} \mathbf{v}\|^2 + \|\mathbf{v}\|_{0,\alpha}^2 + \frac{1}{2}\|\nabla q\|_{0,K}^2.$$

If $C_P \leq \frac{1}{2}$, then we choose $\beta = \frac{1}{2}$ and obtain (2.21). If $C_P \geq \frac{1}{2}$, then choosing $\beta > 0$, such that $1 - 2C_P + \beta = \frac{1}{2}$, we derive the lower bound for $\mathcal{A}^{LS}(\mathbf{v}, q; \mathbf{v}, q)$ with $(4C_P - 1)/(4C_P + 1)$, which obviously is greater or equal to $\frac{1}{3}$. Thus we have the desired bound (2.21). \square

Remark 2.2. *We stress that, under the assumption (2.7) and the choice of the norms in the spaces \mathbf{V} and W , the coercivity constant of the bilinear form in the least-squares formulation does not depend on the contrast κ .*

3. FEM APPROXIMATIONS

3.1. Finite element partitioning and spaces. We assume that the domain Ω is connected and is triangulated with d dimensional simplices. The triangulation is denoted by \mathcal{T}_h and we assume that the simplices forming \mathcal{T}_h are shape regular (the ratio between the diameter of a simplex and the inscribed ball is bounded above). Now we consider the finite element approximation of the problem (1.1a) – (1.1d) using the finite dimensional spaces $\mathbf{V}_h \subset \mathbf{V}$ and $W_h \subset W$ of piece-wise polynomial functions.

It is well known that for the vector variable \mathbf{u} we can use $\mathbf{H}(\text{div})$ -conforming or Raviart-Thomas space \mathcal{RT}_k or Brezzi-Douglas-Marini \mathcal{BDM}_{k+1} finite elements. However, since we have a problem with low regularity it is natural to use the lowest order finite element spaces. For the vector variable \mathbf{u} we use the standard Raviart-Thomas \mathcal{RT}_0 for simplices and cubes. In the case of simplices we can apply also Brezzi-Douglas-Marini \mathcal{BDM}_1 finite elements.

For the two formulations, least-squares and mixed, we use W -conforming finite elements spaces for pressure p . Note that for the least-squares formulation $W = H_D^1(\Omega)$ while for the mixed formulation $W = L^2(\Omega)$. For both cases we show that the corresponding finite element methods are stable uniformly with respect to the contrast κ .

3.2. Mixed FEM and its stability. Thus, we take

$$(3.1) \quad \mathbf{V}_h = \{\mathbf{v} \in \mathbf{V} : \mathbf{v}|_T \in \mathcal{RT}_0 \text{ for } T \in \mathcal{T}_h\}$$

and

$$(3.2) \quad W_h = \{q \in L^2(\Omega) : q|_T \in \mathcal{P}_0, \text{ i.e. } q \text{ is a piece-wise constant function on } \mathcal{T}_h\}.$$

The mixed finite element approximation of the problem (1.1a) – (1.1d) is: find $\mathbf{u}_h \in \mathbf{V}_h$ and $p_h \in W_h$ such that

$$(3.3) \quad \mathcal{A}^{DM}(\mathbf{u}_h, p_h; \mathbf{v}, q) = (f, q), \quad \text{for all } (\mathbf{v}, q) \in \mathbf{V}_h \times W_h,$$

where the bilinear form $\mathcal{A}^{DM}(\mathbf{u}_h, p_h; \mathbf{v}, q)$ is defined by (2.11). Our goal is to prove the discrete variant of the *inf-sup* condition.

Lemma 3.1. *Let \mathbf{V}_h be the space defined by (3.1) and W_h be the space defined by (3.2). Then independently of the contrast κ and the step-size h the following inequality holds true:*

$$(3.4) \quad \inf_{q_h \in W_h} \sup_{\mathbf{v}_h \in \mathbf{V}_h} \frac{(\text{div } \mathbf{v}_h, q_h)}{\|\mathbf{v}_h\|_{\Lambda_\alpha} \|q_h\|} \geq \gamma > 0.$$

Proof. This is stated and proved as Theorem A.2 in the Appendix. \square

As a consequence of Lemma 3.1 and (2.15) we have

Theorem 3.1. *The following bounds are valid for all $\mathbf{u} \in \mathbf{V}_h$ and $p \in W_h$:*

$$(3.5) \quad \alpha_0 (\|\mathbf{u}\|_{\Lambda_\alpha}^2 + \|p\|^2)^{\frac{1}{2}} \leq \sup_{\mathbf{v} \in \mathbf{V}_h, q \in W_h} \frac{\mathcal{A}^{DM}(\mathbf{u}, p; \mathbf{v}, q)}{(\|\mathbf{v}\|_{\Lambda_\alpha}^2 + \|q\|^2)^{\frac{1}{2}}} \leq (\|\mathbf{u}\|_{\Lambda_\alpha}^2 + \|p\|^2)^{\frac{1}{2}}.$$

The constant α_0 may depend on the shape regularity of the mesh, but is independent of the contrast κ and the mesh-size h .

3.3. Least-squares FEM and its stability. For the least-squares formulation the space W_h for the pressure p consists of standard conforming Lagrangian finite elements involving linear polynomials \mathcal{P}_1 (on triangles) and bilinear polynomials \mathcal{Q}_1 (on rectangles).

Since in this case we have conforming spaces, then the results of Lemma 2.2 are valid so that finite element method is stable. Thus we have

Theorem 3.2. *The bilinear form $\mathcal{A}^{LS}(\mathbf{u}, p; \mathbf{v}, q)$ is coercive and bounded on $\mathbf{V}_h \times W_h$ so that the following bounds are valid for all $\mathbf{v} \in \mathbf{V}_h$ and $q \in W_h$:*

$$(3.6) \quad \frac{1}{3}(\|\mathbf{v}\|_{\Lambda_\alpha}^2 + \|q\|_{1,K}^2) \leq \mathcal{A}^{LS}(\mathbf{v}, q; \mathbf{v}, q)$$

and

$$(3.7) \quad \mathcal{A}^{LS}(\mathbf{u}, p; \mathbf{v}, q) \leq 2(\|\mathbf{u}\|_{\Lambda_\alpha}^2 + \|p\|_{1,K}^2)^{\frac{1}{2}}(\|\mathbf{v}\|_{\Lambda_\alpha}^2 + \|q\|_{1,K}^2)^{\frac{1}{2}}.$$

We note that the coercivity and the stability of the least-squares FEM immediately show that we have an efficient preconditioner for this problem as long as we know how to solve an weighted $\mathbf{H}(\text{div})$ problem and also a scalar elliptic problem. Moreover, since the stiffness matrix resulting from the least-squares FEM is an SPD matrix, such a preconditioner can be used in the conjugate gradient algorithm to obtain an efficient and optimal solution method.

4. PRECONDITIONING

4.1. Block-diagonal preconditioner for the system of the finite element method. Now we consider the problem (2.10) and for definiteness we restrict ourselves to the lowest order Raviart-Thomas mixed finite elements on a rectangular grid. The goal of this section is to develop and justify a preconditioner for the algebraic problem resulting from the Galerkin method (2.10) that is independent of the contrast of the media.

Then (2.10) can be written as an operator equation in $X_h = \mathbf{V}_h \times W_h$. Namely, for $\mathbf{x}_h = (\mathbf{u}_h, p_h)$ we have

$$(4.1) \quad \mathcal{A}_h \mathbf{x}_h = \mathbf{f}_h, \quad \text{for } \mathbf{f}_h = (\mathbf{0}, f_h) \in X_h,$$

where for all $\mathbf{y}_h = (\mathbf{v}_h, q_h) \in X_h$

$$(\mathcal{A}_h \mathbf{x}_h, \mathbf{y}_h) = \mathcal{A}^{DM}(\mathbf{u}_h, p_h; \mathbf{v}_h, q_h) \quad \text{or} \quad (\mathcal{A}_h \mathbf{x}_h, \mathbf{y}_h) = \mathcal{A}^{LS}(\mathbf{u}_h, p_h; \mathbf{v}_h, q_h).$$

Obviously, the operator $\mathcal{A}_h : X_h \rightarrow X_h^*$ is self-adjoint on $X_h = \mathbf{V}_h \times W_h$ and indefinite in the case of dual mixed formulation and positive definite in the case of least-squares approximation.

As it has been shown in [5], the operator norms corresponding to the mixed finite element discretization (2.10)

$$(4.2) \quad \|\mathcal{A}_h\|_{\mathcal{L}(X_h, X_h^*)} \quad \text{and} \quad \|\mathcal{A}_h^{-1}\|_{\mathcal{L}(X_h^*, X_h)} \quad \text{are uniformly bounded.}$$

The same is valid for the operator norms corresponding to the least squares formulation.

Now our goal is to construct a positive definite self-adjoint operator $\mathcal{B}_h : X_h \rightarrow X_h^*$ such that all eigenvalues of $\mathcal{B}_h^{-1} \mathcal{A}_h$ are bounded uniformly independent of h and, what is even more important, independent of the contrast κ . From (4.2) it follows that

$$(4.3) \quad \|\mathcal{B}_h\|_{\mathcal{L}(X_h, X_h^*)} \quad \text{and} \quad \|\mathcal{B}_h^{-1}\|_{\mathcal{L}(X_h^*, X_h)} \quad \text{being uniformly bounded in } h \text{ and } \kappa$$

is sufficient for \mathcal{B}_h to be a uniform and robust preconditioner for the minimum residual (MinRes) iteration for the mixed method and conjugate gradient (CG) for the least-squares method.

Let the block-diagonal preconditioner \mathcal{B}_h be defined as

$$(4.4) \quad \mathcal{B}_h := \begin{bmatrix} A_h & 0 \\ 0 & D_h \end{bmatrix}$$

where $A_h : \mathbf{V}_h \rightarrow \mathbf{V}_h^*$ is given by

$$(A_h \mathbf{u}_h, \mathbf{v}_h) := \Lambda_\alpha(\mathbf{u}_h, \mathbf{v}_h) = (\alpha \mathbf{u}_h, \mathbf{v}_h) + (\nabla \cdot \mathbf{u}_h, \nabla \cdot \mathbf{v}_h)$$

and $D_h : W_h \rightarrow W_h^*$ is either I_h , the identity on W_h (for the mixed method) or is defined by the relation $(D_h p_h, q_h) = (K \nabla p_h, \nabla q_h)$ for the least-squares finite element method.

Remark 4.1. *As easily seen, preconditioning is an equivalence relation,*

that is, if $Z_1 \approx Z_2$ and $Z_2 \approx Z_3$ for some operators Z_1, Z_2 and Z_3 , then $Z_1 \approx Z_3$. Therefore, uniform condition number estimates for \mathcal{B}_h , directly carry over to the case when \mathcal{B}_h is replaced by any of its uniform (with respect to the contrast κ and with respect to the mesh size h) preconditioners.

Then condition (4.3) reduces to $\|A_h\|_{\mathcal{L}(\mathbf{V}_h, \mathbf{V}_h^*)}$ and $\|A_h^{-1}\|_{\mathcal{L}(\mathbf{V}_h^*, \mathbf{V}_h)}$ being uniformly bounded in h and κ , which in the case of the mixed method is sufficient for optimality of the preconditioner, see [1]. For the case of the least-squares formulation (4.3) we also need uniform boundedness of $\|D_h\|_{\mathcal{L}(W_h, W_h^*)}$ and $\|D_h^{-1}\|_{\mathcal{L}(W_h^*, W_h)}$. Optimal preconditioners using multigrid and domain decomposition methods for solving the system $D_h p_h = c_h$ have been developed by many authors in the last three decades. One approach for the solution of $D_h p_h = c_h$ (which is, in some sense, the closest one to our work) is the multilevel and auxiliary space multigrid methods proposed in [8, 9].

Thus, the main task in this section is the development and study of a robust and uniformly convergent (with respect to h and κ) iterative method for solving systems with $A_h \mathbf{u}_h = \mathbf{b}_h$.

4.2. Reformulation of the FE problem using matrix notation. The derivation and the justification of the preconditioner will be in the framework of algebraic multilevel/multigrid methods. As a first step we rewrite the operator equation (4.1) in a matrix form. For doing this, instead of functions $\mathbf{x}_h = (\mathbf{u}_h, p_h) \in \mathbf{V}_h \times W_h$ we use the vectors consisting of the degrees of freedom determining \mathbf{x}_h through the nodal basis functions, namely,

$$\mathbf{x} = \begin{bmatrix} \mathbf{u} \\ \mathbf{p} \end{bmatrix}, \quad \text{where} \quad \mathbf{u} \in \mathbb{R}^{|\mathcal{E}_h|}, \quad \mathbf{p} \in \mathbb{R}^{|\mathcal{T}_h|}, \quad \text{are vector columns}$$

and $|\mathcal{E}_h|$ is the number of edges in \mathcal{E}_h , excluding those on Γ_N , and $|\mathcal{T}_h|$ is the number of rectangles of the partition \mathcal{T}_h . Then $A, B_{\text{div}}, \tilde{A}, R$, denote matrices being either square or rectangular. As a result of this convention the equation (4.1) can be written in a matrix form for mixed and least-squares approximations, correspondingly,

$$(4.5) \quad \begin{bmatrix} M_\alpha & -B_{\text{div}}^T \\ -B_{\text{div}} & 0 \end{bmatrix} \begin{bmatrix} \mathbf{u} \\ \mathbf{p} \end{bmatrix} = \begin{bmatrix} \mathbf{0} \\ \mathbf{f} \end{bmatrix}, \quad \begin{bmatrix} A & B_{\text{div}}^T \\ B_{\text{div}} & D \end{bmatrix} \begin{bmatrix} \mathbf{u} \\ \mathbf{p} \end{bmatrix} = \begin{bmatrix} \mathbf{0} \\ \mathbf{f} \end{bmatrix},$$

where $\mathbf{v}^T M_\alpha \mathbf{u} = (\alpha \mathbf{u}_h, \mathbf{v}_h)$, $\mathbf{v}^T B_{\text{div}}^T \mathbf{p} = (p_h, \text{div } \mathbf{v}_h)$, $\mathbf{q}^T B_{\text{div}} \mathbf{u} = (\text{div } \mathbf{u}_h, q_h)$, $\mathbf{v}^T A \mathbf{u} = \Lambda_\alpha(\mathbf{u}_h, \mathbf{v}_h)$, and $\mathbf{q}^T D \mathbf{p} = (K \nabla p_h, \nabla q_h)$. Our aim now is to derive and study a preconditioner for the algebraic system (4.5), which due to the above considerations reduces to efficient preconditioning of the system

$$(4.6) \quad A \mathbf{u} = \mathbf{b}, \quad \mathbf{u}, \mathbf{b} \in \mathbb{R}^N, \quad N := |\mathcal{E}_h|.$$

4.3. Robust preconditioning of the weighted $\mathbf{H}(\text{div})$ -norm. The preconditioning technique described in this section is based on additive Schur complement approximation (ASCA), see, [8]. For the sake of self-containedness, first we will recall the auxiliary space two-grid and multigrid methods that have recently been introduced in [9]. Then we formulate two variants of the algorithm resulting from ASCA that are subject to numerical testing in Section 5.

4.3.1. *Auxiliary space two-grid preconditioner.* The first step in the construction of the preconditioner involves a covering Ω by n overlapping subdomains Ω_i , i.e.,

$$\overline{\Omega} = \bigcup_{i=1}^n \overline{\Omega}_i.$$

This overlapping covering of Ω is to some extent arbitrary with generous overlap. For practical purposes however, we consider the situation shown on Figure 1. In this particular case any finite element in the partition \mathcal{T}_h will belong to no more than four subdomains. We associate subdomain matrices A_i , $i = 1, \dots, n$ with the subdomains Ω_i and assume that they have the following assembling property

$$A = \sum_{i=1}^n R_i^T A_i R_i,$$

where R_i is a rectangular matrix that extends by zero the vector associated with the degrees of freedom of \mathbf{u}_h in Ω_i to a vector representing the degrees of freedom in the whole domain Ω . Assume further that the set \mathcal{D} of degrees of freedom (DOF) of \mathbf{u}_h is partitioned into a set \mathcal{D}_f , fine DOF, and a set \mathcal{D}_c , coarse DOF, so that

$$(4.7) \quad \mathcal{D} = \mathcal{D}_f \oplus \mathcal{D}_c,$$

where $N_1 := |\mathcal{D}_f|$ and $N_2 := |\mathcal{D}_c|$ denote the cardinalities of \mathcal{D}_f and \mathcal{D}_c , respectively, with $N_1 + N_2 = N := |\mathcal{E}_h|$. Recall that $|\mathcal{E}_h|$ is the number of edges in the partitioning \mathcal{T}_h with the edges on Γ_N excluded. Such splitting is not obvious for the mixed finite element method and will be explained in detail later. The splitting (4.7) induces a representation of the matrices A and A_i into two-by-two block form, i.e.,

$$(4.8) \quad A = \begin{bmatrix} A_{11} & A_{12} \\ A_{21} & A_{22} \end{bmatrix}, \quad A_i = \begin{bmatrix} A_{i:11} & A_{i:12} \\ A_{i:21} & A_{i:22} \end{bmatrix}, \quad i = 1, \dots, n.$$

We now introduce the following auxiliary domain decomposition matrix

$$(4.9) \quad \tilde{A} = \begin{bmatrix} A_{1:11} & & & A_{1:12}R_{1:2} \\ & A_{2:11} & & A_{2:12}R_{2:2} \\ & & \ddots & \vdots \\ & & & A_{n:11} & A_{n:12}R_{n:2} \\ R_{1:2}^T A_{1:21} & R_{2:2}^T A_{2:21} & \dots & R_{n:2}^T A_{n:21} & \sum_{i=1}^n R_{i:2}^T A_{i:22} R_{i:2} \end{bmatrix},$$

Setting $\tilde{A}_{11} = \text{diag}\{A_{1:11}, \dots, A_{n:11}\}$, $\tilde{A}_{22} = \sum_{i=1}^n R_{i:2}^T A_{i:22} R_{i:2}$ we have

$$(4.10) \quad \tilde{A} = \begin{bmatrix} \tilde{A}_{11} & \tilde{A}_{12} \\ \tilde{A}_{21} & \tilde{A}_{22} \end{bmatrix}.$$

Note that if A is an SPD matrix then \tilde{A} is a symmetric and positive semi-definite matrix. Moreover, $A \in \mathbb{R}^{N \times N}$ and $\tilde{A} \in \mathbb{R}^{\tilde{N} \times \tilde{N}}$ are related via

$$(4.11) \quad A = R \tilde{A} R^T$$

where

$$(4.12) \quad R = \begin{bmatrix} R_1 & 0 \\ 0 & I_2 \end{bmatrix}, \quad R_1^T = \begin{bmatrix} R_{1:1} \\ R_{2:1} \\ \vdots \\ R_{n:1} \end{bmatrix}.$$

Definition 4.1 (cf. [8]). *The additive Schur complement approximation (ASCA) of the exact Schur complement $S = A_{22} - A_{21}A_{11}^{-1}A_{12}$ is denoted by Q and defined as the Schur complement of \tilde{A} , i.e.,*

$$Q := \tilde{A}_{22} - \tilde{A}_{21}\tilde{A}_{11}^{-1}\tilde{A}_{12} = \sum_{i=1}^n R_{i:2}^T (A_{i:22} - A_{i:21}A_{i:11}^{-1}A_{i:12}) R_{i:2}.$$

Remark 4.2. *Note that $\tilde{A}_{22} = A_{22}$. Thus $\tilde{N}_2 = N_2$ and $\tilde{N}_1 \geq N_1$.*

Next, let $V = \mathbb{R}^N$ and $\tilde{V} = \mathbb{R}^{\tilde{N}}$ and define the surjective mapping $\Pi_{\tilde{D}} : \tilde{V} \rightarrow V$ by

$$(4.13) \quad \Pi_{\tilde{D}} = (R\tilde{D}R^T)^{-1}R\tilde{D},$$

where \tilde{D} is a block-diagonal matrix, e.g.,

$$(4.14) \quad \tilde{D} = \begin{bmatrix} \tilde{D}_{11} & 0 \\ 0 & I \end{bmatrix}$$

where $\tilde{D}_{11} = \tilde{A}_{11}$ or $\tilde{D}_{11} = \text{diag}(\tilde{A}_{11})$.

Then let us consider the following fictitious-space two-grid preconditioner C for A , which is implicitly defined via its inverse

$$(4.15) \quad C^{-1} = \Pi_{\tilde{D}}\tilde{A}^{-1}\Pi_{\tilde{D}}^T.$$

The method of fictitious space preconditioning has first been proposed in [12, 13, 14], and refined in [18] by adding an additional smoother. The basis of the auxiliary space multigrid algorithm, is the following auxiliary space two-grid preconditioner B , which is implicitly defined via its inverse

$$(4.16) \quad B^{-1} := \overline{M}^{-1} + (I - M^{-T}A)C^{-1}(I - AM^{-1})$$

where C is defined according to (4.15), the operator M denotes an A -norm convergent smoother, i.e., $\|I - M^{-1}A\|_A < 1$, and $\overline{M} = M(M + M^T - A)^{-1}M^T$ is the corresponding symmetrized smoother. Examples of such smoothers include the Gauss-Seidel smoother and the damped Jacobi smoother and are well known.

Below in Theorem 4.1 we present an estimate for the condition number under the following assumptions:

(i) the smoother M satisfies for all $\mathbf{v} \in V = \mathbb{R}^N$:

$$(4.17) \quad \underline{c}\langle \mathbf{v}, \mathbf{v} \rangle \leq \rho_A \langle \overline{M}^{-1} \mathbf{v}, \mathbf{v} \rangle \leq \bar{c}\langle \mathbf{v}, \mathbf{v} \rangle,$$

and

$$(4.18) \quad \|M^{-T}A\mathbf{v}\|^2 \leq \frac{\eta}{\rho_A} \|\mathbf{v}\|_A^2,$$

where $\rho_A = \lambda_{\max}(A)$ denotes the spectral radius of A and η is a non-negative constant;

(ii) the operator Π defined by

$$(4.19) \quad \Pi := (I - M^{-T}A)\Pi_{\tilde{D}} = (I - M^{-T}A)(R\tilde{D}R^T)^{-1}R\tilde{D}$$

satisfies the estimate

$$(4.20) \quad \|\Pi\tilde{\mathbf{v}}\|_A^2 \leq c_{\Pi}\|\tilde{\mathbf{v}}\|_{\tilde{A}}^2, \quad \text{for all } \tilde{\mathbf{v}} \in \tilde{V} = \mathbb{R}^{\tilde{N}}.$$

Note that due to $\|\Pi^*\Pi\| = \|\Pi\Pi^*\|$, the bound (4.20) is equivalent to $\|\Pi^*\mathbf{v}\|_{\tilde{A}}^2 \leq c_{\Pi}\|\mathbf{v}\|_A^2$ for all $\mathbf{v} \in V$, where $\Pi^* = \tilde{A}^{-1}\Pi^T A$ denotes the operator satisfying the identity $\langle \Pi\tilde{\mathbf{u}}, \mathbf{v} \rangle_A = \langle \tilde{\mathbf{u}}, \Pi^*\mathbf{v} \rangle_{\tilde{A}}$ for all $\tilde{\mathbf{u}} \in \tilde{V}, \mathbf{v} \in V$.

Remark 4.3. While the results stated here provide uniform bounds on the condition numbers of the preconditioned systems, it is also straightforward to state similar results for a convergent iterative method. Indeed, if, for a large enough scaling parameter τ , we set $C^{-1} = \tau \Pi_{\tilde{D}} \tilde{A}^{-1} \Pi_{\tilde{D}}^T$, then it holds that the related stationary iterative method is A -norm convergent, namely, $\|I - C^{-1}A\|_A < 1$. To keep the presentation focused on preconditioning, however, we only consider $\tau = 1$.

We are now ready to state the theorem (see [9]) which gives the condition number estimate.

Theorem 4.1 (Condition number estimate [9]). *Under the assumptions (4.17)–(4.20) the two-grid preconditioner B defined in (4.16) and (4.15) satisfies*

$$(4.21) \quad \frac{\underline{c}}{\underline{c} + \eta} \leq \lambda_{\min}(B^{-1}A) \leq \lambda(B^{-1}A) \leq \lambda_{\max}(B^{-1}A) \leq \bar{c} + c_{\Pi},$$

that is, $\kappa(B^{-1}A) \leq (\bar{c} + c_{\Pi})(\underline{c} + \eta)/\underline{c}$.

Next, we note that if no smoothing is applied, i.e. $B = C$, then the condition number estimate provided in Theorem 4.1 also holds and we have the following result.

Corollary 4.1. *If $B = C$ and under the assumptions of Theorem 4.1 we have the estimate*

$$(4.22) \quad \kappa(B^{-1}A) \leq c_{\Pi} = c = \|\pi_{\tilde{D}}\|_{\tilde{A}}^2, \quad \text{where} \quad \pi_{\tilde{D}} := R^T \Pi_{\tilde{D}}.$$

4.3.2. Auxiliary space multigrid method. Let $k = 0, 1, \dots, \ell - 1$ be the index of mesh refinement where $k = 0$ corresponds to the finest mesh, i.e., $A^{(0)} := A_h = A$ denotes the fine-grid matrix. Consider the sequence of auxiliary space stiffness matrices $\tilde{A}^{(k)}$, in the two-by-two block factorized form

$$(4.23) \quad (\tilde{A}^{(k)})^{-1} = (\tilde{L}^{(k)})^T \tilde{D}^{(k)} \tilde{L}^{(k)},$$

where

$$(4.24) \quad \tilde{L}^{(k)} = \begin{bmatrix} I & \\ -\tilde{A}_{21}^{(k)}(\tilde{A}_{11}^{(k)})^{-1} & I \end{bmatrix}, \quad \tilde{D}^{(k)} = \begin{bmatrix} (\tilde{A}_{11}^{(k)})^{-1} & \\ & Q^{(k)-1} \end{bmatrix}$$

and the additive Schur complement approximation $Q^{(k)}$ defines the next coarser level matrix, i.e.

$$(4.25) \quad A^{(k+1)} := Q^{(k)}.$$

The algebraic multilevel iteration (AMLI)-cycle auxiliary space multigrid (ASMG) preconditioner $B^{(k)}$ approximating $A^{(k)}$ is defined on all levels $k < \ell$ via the following relations (see [9])

$$(4.26) \quad B^{(k)-1} := \overline{M}^{(k)-1} + (I - M^{(k)-T} A^{(k)}) \Pi^{(k)} (\tilde{L}^{(k)})^T \overline{D}^{(k)} \tilde{L}^{(k)} \Pi^{(k)T} (I - A^{(k)} M^{(k)-1}),$$

where

$$(4.27) \quad \overline{D}^{(k)} := \begin{bmatrix} (\tilde{A}_{11}^{(k)})^{-1} & \\ & B_{\nu}^{(k+1)} \end{bmatrix}$$

and $B_{\nu}^{(k+1)}$ is an approximation of the inverse of the coarse-level matrix, i.e., $B_{\nu}^{(k+1)} \approx A^{(k+1)-1}$,

$$(4.28) \quad B_{\nu}^{(\ell)} := A^{(\ell)-1}.$$

In the linear AMLI-cycle $B_{\nu}^{(k+1)}$ is a polynomial approximation of $A^{(k+1)-1}$, i.e.

$$\begin{aligned} B_{\nu}^{(k+1)} &:= (I - p^{(k)}(B^{(k+1)-1} A^{(k+1)})) A^{(k+1)-1} \\ &=: q^{(k)}(B^{(k+1)-1} A^{(k+1)}) B^{(k+1)-1} \end{aligned}$$

that requires the action of $B^{(k+1)^{-1}}$. The classical choice of $p^{(k)}(t)$ is a scaled and shifted Chebyshev polynomial of degree $\nu_k = \nu$ where

$$p^{(k)}(0) = 1, \quad q^{(k)}(t) := \frac{1 - p^{(k)}(t)}{t} \approx \frac{1}{t}.$$

Other polynomial approximations are possible, e.g., choosing $q^{(k)}(t)$ to be the best approximation to $1/t$ in uniform norm, see [11].

In case of the nonlinear AMLI-cycle ASMG method

$$B_\nu^{(k+1)} = B_\nu^{(k+1)}[\cdot]$$

is a nonlinear mapping whose action on a vector \mathbf{d} is realized by ν iterations of a preconditioned Krylov subspace method. In the following the generalized conjugate gradient method will serve this purpose and hence we denote $B_\nu^{(k+1)}[\cdot] = B_{\text{GCG},\nu}^{(k+1)}[\cdot]$.

An important step in the construction is that performing $B_\nu^{(k+1)}[\cdot]$ one applies (4.26) also for preconditioning at level $(k+1)$. Hence, (4.26) becomes a nonlinear operator, too—we will therefore write

$$B^{(k)^{-1}} = B^{(k)^{-1}}[\cdot], \quad \text{for all } k < \ell.$$

4.3.3. Nonlinear ASMG algorithms. In the remainder of this section we will present two variants of nonlinear ASMG algorithms for preconditioning the SPD matrices arising from discretization of the weighted bilinear form (2.6) and comment on some details of their implementation in the specific situation of using lowest-order Raviart-Thomas elements on rectangles.

On Figure 1 we give an illustration of the *covering of Ω* by overlapping subdomains, these are 9 staggered subdomains each of size $1/2$ of the original domain Ω .

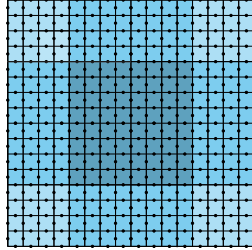


FIGURE 1. Covering of the domain by nine overlapping subdomains

Next, let us comment on the *partitioning* (4.7) of the set \mathcal{D} of DOF. We illustrate it in case of two grids coarse, \mathcal{T}_H , and fine, \mathcal{T}_h , where $H = 2h$. Then the corresponding sets of the edges are \mathcal{E}_H and \mathcal{E}_h . The following relations are obvious: $4|\mathcal{T}_H| = |\mathcal{T}_h|$ and $2|\mathcal{E}_H| + 4|\mathcal{T}_H| = |\mathcal{E}_h|$. Since in the setting of the lowest-order Raviart-Thomas finite elements it is not immediately clear how to partition \mathcal{D} , we perform a preprocessing step which consists of a *compatible two-level basis transformation*, see e.g. [8]. The global matrix A is transformed according to

$$(4.29) \quad \hat{A} = J^T A J, \quad \hat{A}, J, A \in \mathbb{R}^{|\mathcal{E}_h| \times |\mathcal{E}_h|},$$

where the transformation matrix J is the product of a permutation matrix P and another transformation matrix J_\pm , i.e.

$$(4.30) \quad J = P J_\pm, \quad P, J_\pm \in \mathbb{R}^{|\mathcal{E}_h| \times |\mathcal{E}_h|}.$$

The permutation P allows us to provide a two-level numbering of the DOF that splits them into two groups, the first one consisting of DOF associated with fine-grid edges that are not part of any coarse-grid edge (interior DOF) and the second one keeping all remaining DOF ordered such that

any two that are on one edge have consecutive numbers. The transformation matrix J_{\pm} in (4.30) is of the form

$$J_{\pm} = \begin{bmatrix} I & \\ & J_{22} \end{bmatrix}, \quad \text{where } I \in \mathbb{R}^{(4|\mathcal{T}_H|) \times (4|\mathcal{T}_H|)},$$

J_{22} has the form

$$J_{22} = \frac{1}{2} \begin{bmatrix} 1 & -1 & & & & & & \\ & & 1 & -1 & & & & \\ & & & & \ddots & \ddots & & \\ & & & & & & -1 & 1 \\ 1 & 1 & & & & & & \\ & & 1 & 1 & & & & \\ & & & & \ddots & \ddots & & \\ & & & & & & 1 & 1 \end{bmatrix}, \quad \text{where } J_{22} \in \mathbb{R}^{(2|\mathcal{E}_H|) \times (2|\mathcal{E}_H|)}.$$

The analogous transformation is performed on a local level on each subdomain Ω_i , i.e.

$$(4.31) \quad \hat{A}_i = J_i^T A_i J_i,$$

where again $J_i = P_i J_{\pm,i}$ with P_i the permutation explained above but performed on the degrees of freedom in the subdomain Ω_i and $J_{\pm,i}$ has the same meaning but restricted to the subdomain Ω_i .

Definition 4.2. *The global and local transformations will be called compatible if*

$$(4.32) \quad \hat{A} = J^T A J = \sum_{i=1}^{n_G} \hat{R}_i^T \hat{A}_i \hat{R}_i$$

which is equivalent to

$$(4.33) \quad R_i J = J_i \hat{R}_i.$$

The introduced transformation matrix J defines the splitting of the DOF into coarse and fine, namely the FDOF correspond to the set of interior DOF and half differences on the coarse edges while the CDOF correspond to the half sums on the coarse edges.

Finally we formulate the following two algorithms (variants of nonlinear ASMG) for solving linear systems with the matrix A resulting from discretization of (2.6).

The first algorithm applies the nonlinear ASMG method in the two-level basis, i.e., all matrices $A^{(k)}$ are transformed into two-level basis, i.e.,

$$\hat{A}^{(k)} = J^{(k)T} A^{(k)} J^{(k)}, \quad \text{for all } k < \ell$$

and also the smoothing is performed in the two-level basis, i.e., using \hat{M} instead of M .

Algorithm 4.1. *Nonlinear ASMG method–Variant I: Action of (4.26) on a vector $\hat{\mathbf{d}}$*

<i>Pre-smoothing:</i>	$\hat{\mathbf{u}} = (\hat{M}^{(k)})^{-1} \hat{\mathbf{d}}$
<i>Auxiliary space correction:</i>	$\left\{ \begin{array}{l} \begin{pmatrix} \tilde{\mathbf{q}}_1 \\ \tilde{\mathbf{q}}_2 \end{pmatrix} := \tilde{\mathbf{q}} = \Pi_{\tilde{D}^{(k)}}^T (\hat{\mathbf{d}} - \hat{A}^{(k)} \hat{\mathbf{u}}) \\ \tilde{\mathbf{p}}_1 = (\tilde{A}_{11}^{(k)})^{-1} \tilde{\mathbf{q}}_1 \\ \tilde{\mathbf{p}}_2 = J^{(k+1)} B_{\text{GCG}, \nu}^{(k+1)} [J^{(k+1)T} (\tilde{\mathbf{q}}_2 - \tilde{A}_{21}^{(k)} \tilde{\mathbf{p}}_1)] \\ \tilde{\mathbf{q}}_1 = \tilde{\mathbf{p}}_1 - (\tilde{A}_{11}^{(k)})^{-1} \tilde{A}_{12}^{(k)} \tilde{\mathbf{p}}_2 \\ \tilde{\mathbf{q}}_2 = \tilde{\mathbf{p}}_2 \\ \tilde{\mathbf{v}} = \hat{\mathbf{u}} + \Pi_{\tilde{D}^{(k)}} \tilde{\mathbf{q}} \end{array} \right.$
<i>Post-smoothing:</i>	$(\hat{B}^{(k)})^{-1} [\hat{\mathbf{d}}] := \hat{\mathbf{v}} + (\hat{M}^{(k)})^{-T} (\hat{\mathbf{d}} - \hat{A}^{(k)} \hat{\mathbf{v}})$

The second algorithm applies the nonlinear ASMG method directly in the original basis of standard Raviart-Thomas basis functions and reads as follows.

Algorithm 4.2. *Nonlinear ASMG method–Variant II: Action of (4.26) on a vector \mathbf{d}*

<i>Pre-smoothing:</i>	$\mathbf{u} = M^{(k)-1} \mathbf{d}$
<i>Auxiliary space correction:</i>	$\left\{ \begin{array}{l} \begin{pmatrix} \tilde{\mathbf{q}}_1 \\ \tilde{\mathbf{q}}_2 \end{pmatrix} := \tilde{\mathbf{q}} = \Pi_{\tilde{D}^{(k)}}^T J^{(k)T} (\mathbf{d} - A^{(k)} \mathbf{u}) \\ \tilde{\mathbf{p}}_1 = (\tilde{A}_{11}^{(k)})^{-1} \tilde{\mathbf{q}}_1 \\ \tilde{\mathbf{p}}_2 = B_{\text{GCG}, \nu}^{(k+1)} [(\tilde{\mathbf{q}}_2 - \tilde{A}_{21}^{(k)} \tilde{\mathbf{p}}_1)] \\ \tilde{\mathbf{q}}_1 = \tilde{\mathbf{p}}_1 - (\tilde{A}_{11}^{(k)})^{-1} \tilde{A}_{12}^{(k)} \tilde{\mathbf{p}}_2 \\ \tilde{\mathbf{q}}_2 = \tilde{\mathbf{p}}_2 \\ \mathbf{v} = \mathbf{u} + J^{(k)} \Pi_{\tilde{D}^{(k)}} \tilde{\mathbf{q}} \end{array} \right.$
<i>Post-smoothing:</i>	$B^{(k)-1}[\mathbf{d}] := \mathbf{v} + M^{(k)-T} (\mathbf{d} - A^{(k)} \mathbf{v})$

Remark 4.4. Note that the matrices $\tilde{A}_{11}^{(k)}$, $\tilde{A}_{12}^{(k)}$, $\tilde{A}_{21}^{(k)}$ are identical in both algorithms.

Remark 4.5. In general the matrices $\hat{A}^{(k)}$ have slightly more nonzero entries as compared to $A^{(k)}$ and thus Algorithm 4.2 increases computational memory requirements.

Remark 4.6. Considering the two-level preconditioners \hat{B} and B defined according to Algorithm 4.1 and Algorithm 4.2, and assuming that no smoothing is performed, i.e., $\hat{M} = M = 0$, the corresponding condition number bounds for the preconditioned operators in two-level basis and standard basis read $\kappa(\hat{B}^{-1} \hat{A}) \leq \|R^T \Pi_{\tilde{D}}\|_{\tilde{A}}^2$ and $\kappa(B^{-1} A) \leq \|R^T J \Pi_{\tilde{D}}\|_{\tilde{A}}^2$.

5. NUMERICAL EXPERIMENTS

5.1. Description of the parameters and the numerical test examples. Subject to numerical testing are three representative cases of problems characterized by a highly varying coefficient $\alpha(x) = K^{-1}(x)$, namely:

- [a] A binary distribution of the coefficient described by islands on which $\alpha = 1.0$ against a background where $\alpha = 10^{-q}$, see Figure 2;
- [b] Inclusions with $\alpha = 1.0$ and a background with a coefficient $\alpha = \alpha_T = 10^{-q_{\text{rand}}}$ that is constant on each element $\tau \in \mathcal{T}_h$, where the random integer exponent $q_{\text{rand}} \in \{0, 1, 2, \dots, q\}$ is uniformly distributed, see Figure 3;
- [c] Three two-dimensional slices of the SPE10 (Society of Petroleum Engineers) benchmark problem, see [7], where the contrast κ is 10^7 for slices 44 and 74 and 10^6 for slice 54, see Figure 4.

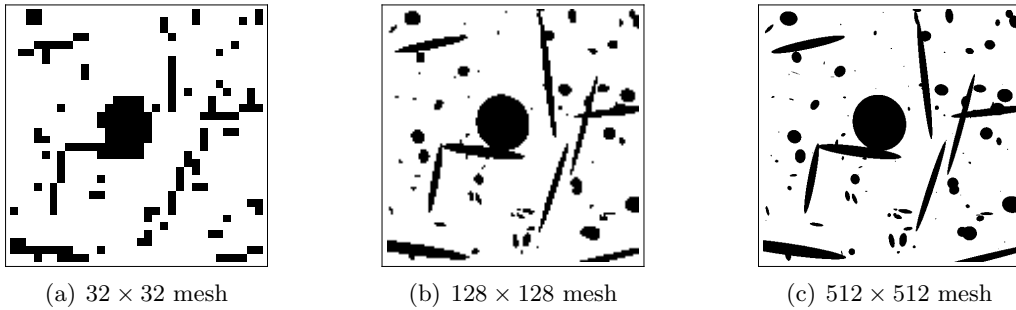


FIGURE 2. Binary distribution of the permeability $K(x)$ corresponding to test case [a]

The numerical experiments are performed over a uniform mesh consisting of $N \times N$ elements (squares) where $N = 4, 8, \dots, 512$, i.e. up to 525312 velocity DOF and 262144 pressure DOF. We have used a direct method to solve the problems on the coarsest grid. The iterative process has been initialized with a random vector. Its convergence has been tested for linear systems with right-hand side zero. We have used overlapping coverings of the domain as shown in Figure 1, where the subdomains are composed of 8×8 elements and overlap with half of their width/height. In the presentation of results we use the following notations:

- ℓ denotes the number of levels;
- $q = \frac{\log \kappa}{\log 10}$ is the logarithm of the contrast κ ;
- n_{ASMG} is the number of auxiliary space multigrid iterations;
- $m \geq 0$ is the number of point Gauss-Seidel pre- and post-smoothing steps;
- ρ is the average convergence factor defined by

$$(5.1) \quad \rho = \left(\frac{\|u_{n_{ASMG}}\|}{\|u_0\|} \right)^{1/n_{ASMG}},$$

where $u_{n_{ASMG}}$ is the first iterate (approximate solution of (4.6)) for which the residual has decreased by a factor of at least 10^8 .

The matrix \tilde{D} is as in (4.14) where $\tilde{D}_{11} = \tilde{A}_{11}$. This choice of \tilde{D} requires an additional preconditioner for the iterative solution of linear systems with the matrix $D = R\tilde{D}R^T$, which is part of the efficient application of the operator $\Pi_{\tilde{D}}$. The systems with D are solved using the preconditioned conjugate gradient (PCG) method. The stopping criterion for this inner iterative process is a residual reduction by a factor 10^6 , the number of PCG iterations to reach it—where reported—is denoted by n_i . A robust and uniform preconditioner B_{ILUE} for D can be constructed based on incomplete

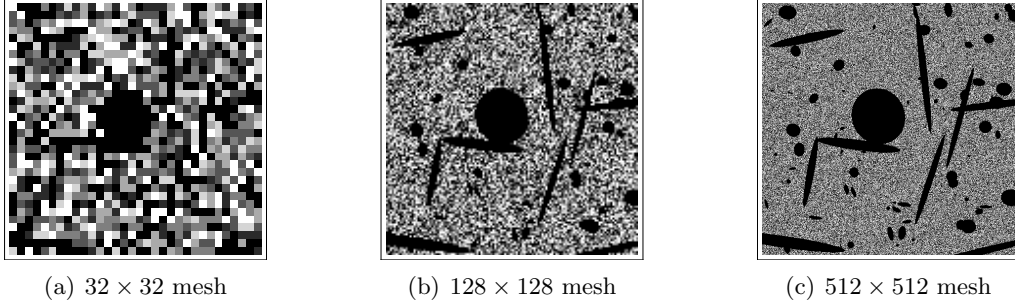


FIGURE 3. Random distribution of $\alpha = K^{-1}(x)$ corresponding to test case [b]

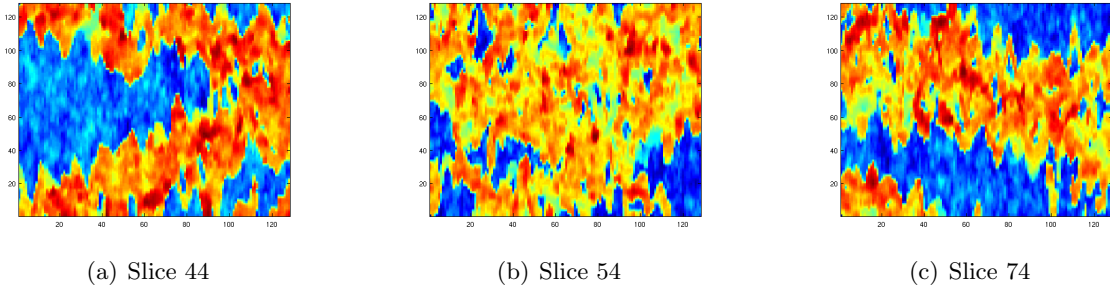


FIGURE 4. Distributions of the permeability $K(x)$ along planes $x_3 = 44, 54, 74$ from the benchmark SPE10 on a 128×128 mesh

factorization using exact local factorization (ILUE). The definition of B_{ILUE} is as follows:

$$B_{ILUE} := LU, \quad U := \sum_{i=1}^n R_i^T U_i R_i, \quad L := U^T \text{diag}(U)^{-1},$$

where

$$D_i = L_i U_i, \quad D = \sum_{i=1}^n R_i^T D_i R_i, \quad \text{diag}(L_i) = I,$$

for details see [10]. Note that as D_i are the local contributions to D related to the subdomains Ω_i , $i = 1, \dots, n$, they are all non-singular.

The next two sections are devoted to the presentation of numerical results. The experiments fall into two categories. The first category, presented in Section 5.2, serves the evaluation of the performance of the ASMG method on linear systems arising from discretization of the weighted $H(\text{div})$ bilinear form (2.6). All three test cases, [a], [b], and [c], are considered and both variants of the ASMG method, Algorithm 4.1 and 4.2, are compared, testing V- and W-cycle with and without smoothing.

The second category of experiments, discussed in Section 5.3, addresses the solution of the indefinite linear system (4.5) arising from problem (2.10) by a preconditioned MinRes method. The main purposes are, on the one hand, to confirm the robustness of the block-diagonal preconditioner (4.4) with respect to arbitrary multiscale coefficient variations, and on the other hand, to demonstrate its numerical scalability.

5.2. Numerical tests for solving the system (4.6). Here we test the ASMG preconditioner for solving the system (4.6) with a matrix corresponding to the discretization of the form $\Lambda_\alpha(\mathbf{u}, \mathbf{v})$.

Example 5.1. The first set of experiments is for the test cases [a] and [b]. In Tables 1–6 we report the number of outer iterations n_{ASMG} for the ℓ -level V-cycle and W-cycle ASMG method defined by Algorithm 4.1. The coarsest mesh is composed of 4×4 squares corresponding to 40 DOF on the \mathcal{RT}_0 space.

ASMG V-cycle: bilinear form (2.6), Algorithm 4.1										
	$\ell = 3$		$\ell = 4$		$\ell = 5$		$\ell = 6$		$\ell = 7$	
	n_{ASMG}	ρ	n_{ASMG}	ρ	n_{ASMG}	ρ	n_{ASMG}	ρ	n_{ASMG}	ρ
$q = 0$	4	0.006	6	0.031	8	0.097	11	0.161	12	0.202
$q = 1$	4	0.005	6	0.034	9	0.115	11	0.169	13	0.224
$q = 2$	4	0.004	6	0.032	10	0.151	12	0.199	13	0.235
$q = 3$	3	0.002	6	0.031	10	0.158	12	0.211	13	0.235
$q = 4$	4	0.004	6	0.041	11	0.157	13	0.213	14	0.256
$q = 5$	4	0.006	7	0.053	11	0.185	16	0.314	19	0.366
$q = 6$	4	0.008	8	0.085	15	0.271	24	0.462	25	0.495

TABLE 1. Example 5.1: case [a] with $K(x) = 10^q$ and no smoothing steps ($m = 0$)

As we can see by comparing the results summarized in Tables 1 and 2 the V-cycle multigrid preconditioner gains robustness with respect to the contrast of a binary distribution of a piecewise constant permeability coefficient when increasing the number of smoothing steps from zero to two. We further observe an increase of the number of ASMG iterations for decreasing mesh size h (in average 2-3 times). At the same time, as seen in Table 3, the W-cycle preconditioner with one smoothing step is robust with respect to both the contrast and the mesh size h .

ASMG V-cycle: bilinear form (2.6), Algorithm 4.1										
	$\ell = 3$		$\ell = 4$		$\ell = 5$		$\ell = 6$		$\ell = 7$	
	n_{ASMG}	ρ	n_{ASMG}	ρ	n_{ASMG}	ρ	n_{ASMG}	ρ	n_{ASMG}	ρ
$q = 0$	4	0.005	5	0.024	6	0.043	8	0.083	8	0.093
$q = 1$	3	0.002	5	0.022	7	0.058	8	0.084	9	0.121
$q = 2$	3	0.002	5	0.019	7	0.068	8	0.091	9	0.121
$q = 3$	3	0.002	5	0.018	7	0.070	8	0.095	9	0.125
$q = 4$	3	0.002	5	0.017	7	0.069	8	0.098	10	0.142
$q = 5$	3	0.002	5	0.017	8	0.082	9	0.118	10	0.145
$q = 6$	4	0.005	4	0.010	8	0.092	9	0.125	11	0.181

TABLE 2. Example 5.1: case [a] with $K(x) = 10^q$ and two smoothing steps ($m = 2$)

ASMG W-cycle: bilinear form (2.6), Algorithm 4.1										
	$\ell = 3$		$\ell = 4$		$\ell = 5$		$\ell = 6$		$\ell = 7$	
	n_{ASMG}	ρ	n_{ASMG}	ρ	n_{ASMG}	ρ	n_{ASMG}	ρ	n_{ASMG}	ρ
$q = 0$	4	0.005	4	0.007	4	0.006	4	0.005	4	0.005
$q = 1$	3	0.002	4	0.007	4	0.007	4	0.005	4	0.004
$q = 2$	3	0.002	5	0.015	5	0.017	4	0.006	3	0.001
$q = 3$	3	0.002	5	0.017	5	0.020	4	0.006	3	0.002
$q = 4$	3	0.002	5	0.016	5	0.019	4	0.005	4	0.005
$q = 5$	3	0.002	4	0.009	6	0.030	4	0.007	4	0.009
$q = 6$	4	0.005	5	0.017	5	0.020	5	0.025	7	0.066

TABLE 3. Example 5.1: case [a], one smoothing step ($m = 1$)

In the next set of numerical experiments we consider the same distribution of inclusions of low permeability as before but this time against a background of a randomly distributed piecewise constant permeability coefficient as shown on Figure 3. The results, presented in Tables 4 and 5, are even better than those obtained for the binary distribution in the sense that here both V - and W -cycle are robust with respect to the contrast.

ASMG V-cycle: bilinear form (2.6), Algorithm 4.1										
	$\ell = 3$		$\ell = 4$		$\ell = 5$		$\ell = 6$		$\ell = 7$	
	n_{ASMG}	ρ	n_{ASMG}	ρ	n_{ASMG}	ρ	n_{ASMG}	ρ	n_{ASMG}	ρ
$q = 0$	4	0.007	6	0.027	9	0.102	10	0.156	12	0.210
$q = 1$	4	0.006	6	0.035	9	0.103	11	0.171	13	0.224
$q = 2$	4	0.005	6	0.032	9	0.102	11	0.159	13	0.222
$q = 3$	4	0.006	6	0.042	9	0.110	11	0.174	13	0.229
$q = 4$	4	0.006	7	0.043	9	0.127	11	0.183	13	0.233
$q = 5$	4	0.006	7	0.049	10	0.138	12	0.195	13	0.239
$q = 6$	4	0.006	7	0.056	10	0.149	12	0.207	14	0.252

TABLE 4. Example 5.1: case [b], no smoothing steps ($m = 0$)

Example 5.2. The second set of experiments is related to the test case [c] where, similarly to Example 5.1, we examine the performance of the preconditioner for the bilinear form (2.6). Here

	$\ell = 3$		$\ell = 4$		$\ell = 5$		$\ell = 6$		$\ell = 7$	
	n_{ASMG}	ρ	n_{ASMG}	ρ	n_{ASMG}	ρ	n_{ASMG}	ρ	n_{ASMG}	ρ
$q = 0$	4	0.005	5	0.024	6	0.046	8	0.083	8	0.091
$q = 1$	4	0.005	6	0.033	7	0.060	8	0.091	9	0.124
$q = 2$	3	0.002	5	0.023	6	0.045	7	0.069	9	0.121
$q = 3$	3	0.002	5	0.021	6	0.043	7	0.071	8	0.100
$q = 4$	4	0.005	5	0.023	6	0.044	8	0.089	9	0.122
$q = 5$	4	0.005	5	0.024	6	0.045	8	0.090	9	0.125
$q = 6$	4	0.005	6	0.034	6	0.045	8	0.091	10	0.142

TABLE 5. Example 5.1: case [b], two smoothing steps ($m = 2$)

ASMG W-cycle: bilinear form (2.6), Algorithm 4.1										
	$\ell = 3$		$\ell = 4$		$\ell = 5$		$\ell = 6$		$\ell = 7$	
	n_{ASMG}	ρ	n_{ASMG}	ρ	n_{ASMG}	ρ	n_{ASMG}	ρ	n_{ASMG}	ρ
$q = 0$	4	0.005	4	0.007	4	0.006	4	0.005	4	0.005
$q = 1$	4	0.006	4	0.007	4	0.007	4	0.006	4	0.005
$q = 2$	4	0.004	4	0.009	5	0.016	4	0.007	4	0.006
$q = 3$	4	0.005	5	0.015	5	0.015	4	0.009	4	0.006
$q = 4$	4	0.005	5	0.016	5	0.016	4	0.009	4	0.008
$q = 5$	4	0.005	5	0.018	5	0.015	4	0.009	4	0.008
$q = 6$	4	0.005	5	0.019	5	0.015	4	0.008	4	0.007

TABLE 6. Example 5.1: case [b], one smoothing step ($m = 1$)

we compare the ASMG preconditioners defined by Algorithm 4.1 and Algorithm 4.2. In this example the finest mesh is always composed of 256×256 elements meaning that changing the number of levels ℓ refers to a different size of the coarse-grid problem. Tables 7–12 report the number of outer iterations n_{ASMG} and the maximum number of inner iterations n_i needed to reduce the residual of the linear systems with the matrix $R\tilde{D}R^T$ by a factor of 10^6 .

Tables 7 and 8 contain the results for SPE10 slice 44. We see that while the number of inner iterations is about the same, the number n_{ASMG} of outer iterations in case of the V-cycle is on average 2.5 times higher than those for the W-cycle. However, since the complexity of the V-cycle is lower, the overall performance of these two methods is comparable. Comparing the two algorithms, we see that they have approximately the same number of inner and outer iterations. Due to its lower memory requirements we could therefore recommend Algorithm 4.1 for these kinds of problems. On Tables 11–12 we present the results for SPE10 slice 74, which has slightly different permeability distribution but has the same contrast, $\kappa = 10^7$. Computational results are pretty much the same for this case as well.

5.3. Testing of block-diagonal preconditioner for system (4.5) within MinRes iteration.

Now we present a number of numerical experiments for solving the mixed finite element system (4.5) by using a preconditioned MinRes method. We consider two different examples, first, Example 5.3 in which the performance of the block-diagonal preconditioner and its dependence on the accuracy of the inner solves with W-cycle ASMG preconditioner is evaluated, and second, Example 5.4 that tests the scalability of the MinRes iteration, again using a W-cycle ASMG preconditioner with one smoothing step for the inner iterations.

ASMG V-cycle: bilinear form (2.6)												
Algorithm 4.1						Algorithm 4.2						
$m = 0$				$m = 1$			$m = 0$			$m = 1$		
n_{ASMG}	ρ	n_i		n_{ASMG}	ρ	n_i	n_{ASMG}	ρ	n_i	n_{ASMG}	ρ	n_i
$\ell = 3$	8	0.080	4	7	0.064	5	8	0.090	5	8	0.080	5
$\ell = 4$	10	0.157	6	9	0.122	6	11	0.184	6	10	0.143	6
$\ell = 5$	12	0.209	6	10	0.154	6	13	0.231	6	11	0.185	6
$\ell = 6$	13	0.239	6	11	0.179	6	14	0.264	6	12	0.207	6
$\ell = 7$	13	0.239	6	11	0.179	6	14	0.264	6	12	0.207	6

TABLE 7. Example 5.2: case [c] - slice 44 of SPE10 benchmark

ASMG W-cycle: bilinear form (2.6)												
Algorithm 4.1						Algorithm 4.2						
$m = 0$				$m = 1$			$m = 0$			$m = 1$		
n_{ASMG}	ρ	n_i		n_{ASMG}	ρ	n_i	n_{ASMG}	ρ	n_i	n_{ASMG}	ρ	n_i
$\ell = 3$	5	0.019	6	5	0.014	5	5	0.025	5	5	0.017	6
$\ell = 4$	5	0.019	6	5	0.014	5	5	0.025	5	5	0.017	6
$\ell = 5$	5	0.019	6	5	0.014	5	6	0.026	6	5	0.017	6
$\ell = 6$	5	0.019	6	5	0.014	5	6	0.026	6	5	0.017	6
$\ell = 7$	5	0.019	6	5	0.014	5	6	0.026	6	5	0.017	6

TABLE 8. Example 5.2: case [c] - slice 44 of SPE10 benchmark

ASMG V-cycle: bilinear form (2.6)												
Algorithm 4.1						Algorithm 4.2						
$m = 0$				$m = 1$			$m = 0$			$m = 1$		
n_{ASMG}	ρ	n_i		n_{ASMG}	ρ	n_i	n_{ASMG}	ρ	n_i	n_{ASMG}	ρ	n_i
$\ell = 3$	7	0.070	4	7	0.059	4	8	0.079	4	7	0.069	4
$\ell = 4$	10	0.156	5	9	0.122	6	11	0.173	5	10	0.143	6
$\ell = 5$	13	0.236	5	11	0.173	6	14	0.256	5	12	0.196	6
$\ell = 6$	14	0.253	5	11	0.183	6	15	0.283	5	12	0.210	6
$\ell = 7$	14	0.253	6	11	0.183	6	15	0.283	5	12	0.210	6

TABLE 9. Example 5.2: case [c] - slice 54 of SPE10 benchmark

Example 5.3. Here we apply the MinRes iteration to solve (4.5) for test case [c]. The hierarchy of meshes is the same as in Example 5.2. An ASMG W-cycle based on Algorithm 4.1 with one smoothing step has been used as a preconditioner on the \mathcal{RT}_0 space. Table 13 shows the number of MinRes iterations denoted by n_{MinRes} , the maximum number of ASMG iterations n_{ASMG} needed to achieve an ASMG residual reduction by ϖ .

Example 5.4. In the last set of experiments the MinRes iteration has been used to solve (4.5) for test case [c] on the same hierarchy of meshes as in Example 5.1. An ASMG W-cycle based on Algorithm 4.1 with one smoothing step has been used as a preconditioner on the \mathcal{RT}_0 space for a residual reduction by 10^8 . Table 14 shows the number of MinRes iterations n_{MinRes} , the maximum number of (inner) ASMG iterations n_{ASMG} per (outer) MinRes iteration, and the number

ASMG W-cycle: bilinear form (2.6)												
Algorithm 4.1						Algorithm 4.2						
$m = 0$				$m = 1$			$m = 0$			$m = 1$		
n_{ASMG}	ρ	n_i		n_{ASMG}	ρ	n_i	n_{ASMG}	ρ	n_i	n_{ASMG}	ρ	n_i
$\ell = 3$	5	0.016	4	5	0.013	4	5	0.021	4	5	0.016	4
$\ell = 4$	5	0.017	6	5	0.013	5	5	0.023	6	5	0.017	6
$\ell = 5$	5	0.018	6	5	0.013	6	5	0.023	6	5	0.017	6
$\ell = 6$	5	0.018	6	5	0.013	6	5	0.023	6	5	0.017	6
$\ell = 7$	5	0.018	6	5	0.013	6	5	0.023	6	5	0.017	6

TABLE 10. Example 5.2: case [c] - slice 54 of SPE10 benchmark

ASMG V-cycle: bilinear form (2.6)												
Algorithm 4.1						Algorithm 4.2						
$m = 0$				$m = 1$			$m = 0$			$m = 1$		
n_{ASMG}	ρ	n_i		n_{ASMG}	ρ	n_i	n_{ASMG}	ρ	n_i	n_{ASMG}	ρ	n_i
$\ell = 3$	8	0.090	4	7	0.070	4	8	0.097	4	8	0.087	4
$\ell = 4$	11	0.178	5	10	0.145	5	12	0.199	5	11	0.162	6
$\ell = 5$	13	0.229	5	11	0.166	6	14	0.257	5	11	0.183	6
$\ell = 6$	13	0.242	6	11	0.180	6	15	0.276	6	13	0.219	6
$\ell = 7$	13	0.242	6	11	0.180	6	15	0.276	6	13	0.219	6

TABLE 11. Example 5.2: case [c] - slice 74 of SPE10 benchmark

ASMG W-cycle: bilinear form (2.6)												
Algorithm 4.1						Algorithm 4.2						
$m = 0$				$m = 1$			$m = 0$			$m = 1$		
n_{ASMG}	ρ	n_i		n_{ASMG}	ρ	n_i	n_{ASMG}	ρ	n_i	n_{ASMG}	ρ	n_i
$\ell = 3$	5	0.019	4	5	0.014	4	5	0.025	4	5	0.017	5
$\ell = 4$	5	0.020	5	5	0.015	5	6	0.030	5	5	0.018	6
$\ell = 5$	5	0.020	6	5	0.015	6	6	0.030	6	5	0.018	6
$\ell = 6$	5	0.020	6	5	0.015	6	6	0.030	6	5	0.018	6
$\ell = 7$	5	0.020	6	5	0.015	6	6	0.030	6	5	0.018	6

TABLE 12. Example 5.2: case [c] - slice 74 of SPE10 benchmark

of DOF. Note that as long as the product $n_{MinRes}n_{ASMG}$ is constant, the total number of arithmetic operations required to achieve any prescribed accuracy is proportional to the number of DOF.

5.4. Some conclusions and general comments regarding the numerical experiments. The presented numerical results clearly demonstrate the efficiency of the proposed algebraic multilevel iteration (AMLI)-cycle auxiliary space multigrid (ASMG) preconditioner for problems with highly varying coefficients as they typically arise in the mathematical modelling of physical processes in high-contrast and high-frequency media.

The first group of tests examines the convergence behavior of the nonlinear ASMG method for the weighted bilinear form (2.6). This is a key point in the presented study. The cases [a] and [b] are designed to represent a typical multiscale geometry with islands and channels. Although case [b] (a

MinRes iteration: saddle point system (4.5)						
	$\varpi = 10^6$		$\varpi = 10^8$		$\varpi = 10^{10}$	
	n_{MinRes}	n_{ASMG}	n_{MinRes}	n_{ASMG}	n_{MinRes}	n_{ASMG}
$\ell = 3$	24	4	17	6	15	8
$\ell = 4$	15	5	13	6	13	8
$\ell = 5$	21	5	17	6	15	8
$\ell = 6$	22	5	17	6	15	8
$\ell = 7$	22	5	17	6	15	8

TABLE 13. Example 5.3: case [c] - slice 44 of SPE10 benchmark. The hierarchy of meshes is the same as in Example 5.2.

MinRes iteration: saddle point system (4.5)			
	n_{MinRes}	n_{ASMG}	DOF
$\ell = 4$	13	5	3,136
$\ell = 5$	13	6	12,416
$\ell = 6$	15	6	49,408
$\ell = 7$	17	6	197,120
$\ell = 8$	17	6	787,456

TABLE 14. Example 5.3: case [c] - slice 44 of SPE10 benchmark. The hierarchy of meshes is the same as in Example 5.1.

background with a random coefficient) appears to be more complicated, the impact of the multiscale heterogeneity seems to be stronger in the binary case [a] where the number of iterations is slightly larger. However, in both cases we observe a uniformly converging ASMG V-cycle with $m = 2$ and W-cycle ($\nu = 2$) with $m = 1$. Some small fluctuations of the results in the right-lower corner of the tables could be due to some round off effects. Case [c] (SPE10) is a popular benchmark problem in the petroleum engineering community. Here we observe robust and uniform convergence with respect to the number of levels ℓ , or, equivalently, mesh-size h . Note that such uniform convergence is present for the ASMG V-cycle even without smoothing iterations (i.e. $m = 0$) and for both, Algorithm 4.1 and Algorithm 4.2. In addition, Algorithm 4.2 is computationally more favorable when compared to Algorithm 4.1 because the matrices used in Algorithm 4.2 have fewer non-zeroes (they are sparser).

The last two tables, Table 13–14, confirm the expected optimal convergence rate of the block-diagonally preconditioned MinRes iteration applied to the coupled saddle point system (4.5). The results in Table 13 demonstrate how the efficiency (in terms of the product $n_{MinRes}n_{ASMG}$) is achieved for a relative accuracy of 10^{-8} of the inner ASMG solver. Table 14 illustrates the scalability of the solver indicated by a (almost) constant number of MinRes and ASMG iterations since the total computational work in terms of fine grid matrix vector multiplications is proportional to the product $n_{MinRes}n_{ASMG}$.

Although not in the scope of this study, we note that the proposed auxiliary space multigrid method would be suitable for implementation on distributed memory computer architectures.

APPENDIX A. DISCRETE INF-SUP CONDITION

Here we provide a proof of the discrete inf-sup condition (3.4) for the bilinear form arising in the mixed finite element method. We begin by introducing some details regarding the finite element spaces involved in the approximation of problem (2.10) or (2.12).

A.1. Raviart-Thomas-Nédélec space. We consider the standard lowest order Raviart-Thomas-Nédélec space \mathbf{V}_h . Recall that every element $\mathbf{v} \in \mathbf{V}_h$ can be written as

$$(A.1) \quad \mathbf{v} = \sum_{e \in \mathcal{E}_h} \sigma_e(\mathbf{v}) \psi_e(\mathbf{x}), \quad \sigma_e(\mathbf{v}) = \int_e \mathbf{v} \cdot \mathbf{n}_e.$$

Here the vector \mathbf{n}_e has a fixed direction (normal to e), and this direction is set once and for all for every face $e \in \mathcal{E}_h$. For an element $T \in \mathcal{T}_h$ let $\mathbf{n}_{e,T}$ define the unit normal vector to $e \in \partial T \cap \mathcal{E}_h$ which points outward with respect to T . Now, if e is the intersection of two elements from \mathcal{T}_h , $e = T_e^+ \cap T_e^-$, then T_e^+ is the element for which $\mathbf{n}_e \cdot \mathbf{n}_{e,T} = 1$ and T_e^- is the element for which $\mathbf{n}_e \cdot \mathbf{n}_{e,T} = -1$. If e is on the boundary of the domain then the corresponding element is T_e^+ and T_e^- is missing. Finally, for a piece-wise constant function $q \in W_h$ we denote

$$q_{\pm,e} = q|_{T_e^{\pm}}, \quad e \in \mathcal{E}_h.$$

The basis function $\psi_e \in \mathbf{V}_h$, for $e \in \mathcal{E}_h$ corresponds to an edge/face $e \in \partial T$, for some $T \in \mathcal{T}_h$. If e is the face opposite to the vertex P_e of the triangle/tetrahedron T , then

$$(A.2) \quad \psi_e|_T = \frac{c_d}{|T|}(\mathbf{x} - \mathbf{x}_{P_e}).$$

where c_d is a constant depending only on the spatial dimension d and is chosen so that $\int_e \psi_e \cdot \mathbf{n}_e = 1$.

We note that explicit formulas similar to (A.2) are available also for the case of lowest order Raviart-Thomas-Nédélec elements on d -dimensional cuboids (parallelograms or rectangular parallelepipeds). Indeed, if a cuboidal element $T \in \mathcal{T}_h$ is with faces parallel to the coordinate planes, this can be seen as follows. We denote by ψ_k^{\pm} , the basis function which corresponds to a face F_k^{\pm} with outward normal vector $\pm \mathbf{e}_k$, $k = 1, \dots, d$. Here, \mathbf{e}_k is the k -th coordinate vector in \mathbb{R}^d . Let $\mathbf{x}_{M,k}^{\pm} \in \mathbb{R}^d$ be the mass center of the face F_k^{\pm} , $k = 1, \dots, d$. We then have

$$(A.3) \quad \psi_k^{\pm}(\mathbf{x}) = \frac{(\mathbf{x} - \mathbf{x}_{M,k}^{\mp})^T \mathbf{e}_k}{|T|} \mathbf{e}_k.$$

Here for simplicity we have used the notation $\mathbf{x}^T \mathbf{e}_k$ for the standard Euclidean inner product of vectors $\mathbf{x}, \mathbf{e}_k \in \mathbb{R}^d$. From this formula we see that over the finite element T the basis functions $\psi_k^{\pm}(\mathbf{x})$ are linear of the variable x_k and constant in the remaining variables in \mathbb{R}^d .

These are exactly $2d$ basis functions satisfying

$$\int_{F_j^{\pm}} \psi_k^+ \cdot \mathbf{n}_{F_j^{\pm}} = \int_{F_k^-} \psi_k^+ \cdot \mathbf{n}_{F_k^-} = 0, \text{ for } j \neq k, \text{ and } \int_{F_k^+} \psi_k^+ \cdot \mathbf{n}_{F_k^+} = 1.$$

with a similar relation for ψ_k^- , $k = 1, \dots, d$. We note that all numerical experiments in the subsequent sections were done using these finite elements.

These simple formulas also show that on a shape regular mesh we have:

$$(A.4) \quad \|\psi_e\|_{0,T}^2 \sim h_e^{2-d}, \quad h_e = \text{diam}(e), \quad T^+ \cap T^- = e \in \mathcal{E}_h.$$

The constants in the norm equivalence in (A.4) depend on the shape of the finite elements, but not on the contrast κ .

We treat Dirichlet, Neumann boundary conditions (or mixture of these) in a unified fashion. In order to do this we set \mathcal{E}_h to denote the set of faces (edges) of \mathcal{T}_h minus the set of faces (edges) on which we have Neumann conditions and $|\mathcal{E}_h|$ is the number of these edges/faces. Thus, in the case of pure Neumann conditions on $\partial\Omega$ the set of faces (edges) \mathcal{E}_h is the set of interior faces (edges). Further, W_h is the space of all piece-wise constant scalar valued functions with zero mean value over Ω , namely, $\int_{\Omega} q = 0$. In the case of pure Dirichlet conditions, W_h is the space of piece-wise constants (without restriction) and \mathcal{E}_h is the set of all faces (edges) in \mathcal{T}_h .

A.2. Scalar products and discrete gradients. We now define a weighted scalar product on \mathbf{V}_h : For a vector of weights $\omega \in \mathbb{R}^{|\mathcal{E}_h|}$ we set

$$(\mathbf{u}, \mathbf{v})_{*,\omega} = \sum_{e \in \mathcal{E}_h} \omega_e \sigma_e(\mathbf{u}) \sigma_e(\mathbf{v}) \|\psi_e\|^2, \quad (\mathbf{u}, \mathbf{v})_{*,1} = \sum_{e \in \mathcal{E}_h} \sigma_e(\mathbf{u}) \sigma_e(\mathbf{v}) \|\psi_e\|^2.$$

Note that $(\mathbf{u}, \mathbf{v})_{*,1}$ is an inner product for which $\omega_e = 1$ for all $e \in \mathcal{E}_h$. The corresponding norms are denoted by $\|\cdot\|_{*,\omega}$ and $\|\cdot\|_{*,1}$.

Next, with the vector $\omega \in \mathbb{R}^{|\mathcal{E}_h|}$, we associate an operator $D_\omega : \mathbf{V}_h \mapsto \mathbf{V}_h$. The action of the operator is determined by defining $\sigma_e(D_\omega \mathbf{v})$ for $e \in \mathcal{E}_h$, since these degrees of freedom uniquely determine any element from \mathbf{V}_h . We set

$$(A.5) \quad \sigma_e(D_\omega \mathbf{v}) = \omega_e \sigma_e(\mathbf{v}).$$

The discrete gradient is defined as adjoint of the “div” in the $(\cdot, \cdot)_{*,1}$ inner product and denoted by “ ∇_h ”. For $q \in W_h$, $\nabla_h q$ is the unique element in \mathbf{V}_h satisfying

$$(A.6) \quad (\mathbf{v}, \nabla_h q)_{*,1} = -(\operatorname{div} \mathbf{v}, q), \quad \text{for all } \mathbf{v} \in \mathbf{V}_h.$$

A straightforward computation (by taking $\mathbf{v} = \psi_e$) shows that

$$\sigma_e(\nabla_h q) = \frac{[q]_e}{\|\psi_e\|^2}, \quad [q]_e = q_{-,e} - q_{+,e}.$$

For Dirichlet boundary faces (edges) $[q]_e = q_{+,e}$. We have the following proposition:

Proposition A.1. *Let $\mathbf{v} \in \mathbf{V}_h$ and $\omega_e > 0$ for all $e \in \mathcal{E}_h$. We then have*

- (i) $(\mathbf{u}, \mathbf{v})_{*,\omega} = (D_\omega \mathbf{u}, \mathbf{v})_{*,1}$;
- (ii) *The bilinear form on $W_h \times W_h$ defined by*

$$(D_\omega \nabla_h \varphi, \nabla_h \chi)_{*,1} = \sum_{e \in \mathcal{E}_h} \frac{\omega_e}{\|\psi_e\|^2} [\varphi]_e [\chi]_e$$

is symmetric and positive definite on W_h .

Proof. (i) follows directly from the definition of D_ω and $(\cdot, \cdot)_{*,\omega}$.

Regarding (ii), we take $\chi = \varphi$ and we obtain

$$(D_\omega \nabla_h \varphi, \nabla_h \varphi)_{*,1} = (\nabla_h \varphi, \nabla_h \varphi)_{*,\omega} = \sum_{e \in \mathcal{E}_h} \frac{\omega_e}{\|\psi_e\|^2} ([\varphi]_e)^2 \geq 0.$$

To show that this inequality is strict (which implies positive definiteness of the bilinear form) we observe that if we have Dirichlet conditions on part of, or, the whole boundary then the matrix corresponding to this bilinear form is a symmetric, weakly diagonally dominant M -matrix and hence it is positive definite. If we have Neumann conditions on $\partial\Omega$, then setting $(\nabla_h \varphi, \nabla_h \varphi)_{*,\omega} = 0$ implies that $q_{+,e} = q_{-,e}$ for all $e \in \mathcal{E}_h$ and we conclude that q is a constant on Ω . Since the average of q is 0 (in case of Neumann conditions) we conclude that $q = 0$. Thus, the bilinear form has a trivial kernel and is positive definite on W_h . The proof of (ii) is complete. \square

A.3. A discrete *a priori* estimate. Recall that $K(x)$ and α are a piece-wise constant tensor-functions whose discontinuities are aligned with the triangulation \mathcal{T}_h . For any face $e \in \mathcal{E}_h$, $e = \overline{T}_e^+ \cap \overline{T}_e^-$ we now define

$$(A.7) \quad \hat{\alpha} \in \mathbb{R}^{|\mathcal{E}_h|}, \quad \hat{\alpha}_e = \frac{\|\psi_e\|_{0,\alpha,T_e^+}^2}{\|\psi_e\|^2} + \frac{\|\psi_e\|_{0,\alpha,T_e^-}^2}{\|\psi_e\|^2}, \quad \hat{\kappa} \in \mathbb{R}^{|\mathcal{E}_h|}, \quad \hat{\kappa}_e = \hat{\alpha}_e^{-1}.$$

We have the following lemma which is a crucial ingredient in the proof of the discrete inf-sup condition.

Lemma A.1. *Let $\hat{\alpha} \in \mathbb{R}^{|\mathcal{E}_h|}$ and $\hat{\kappa} \in \mathbb{R}^{|\mathcal{E}_h|}$ be defined as in (A.7). Then*

- (i) $\|\mathbf{u}\|_{0,\alpha}^2 \leq (d+1)\|\mathbf{u}\|_{*,\hat{\alpha}}^2$ and $\|\mathbf{u}\|^2 \approx \|\mathbf{u}\|_{*,1}^2$.
- (ii) $D_{\hat{\alpha}}D_{\hat{\kappa}} = I$.
- (iii) $\hat{\alpha}_e \leq 2$ and $\hat{\kappa}_e \geq \frac{1}{2}$.

Proof. To prove the first inequality in (i), let $\mathbf{u} \in \mathbf{V}_h$. Then, for all $T \in \mathcal{T}_h$ we have $\mathbf{u}|_T = \sum_{e \in \partial T} \sigma_e(\mathbf{u})\boldsymbol{\psi}_e$, and, hence,

$$\begin{aligned}
\|\mathbf{u}\|_{0,\alpha}^2 &= \sum_T \int_T \alpha_T \mathbf{u} \cdot \mathbf{u} = \sum_T \sum_{e \in \partial T} \sum_{e' \in \partial T} \sigma_e(\mathbf{u})\sigma_{e'}(\mathbf{u}) \int_T \alpha_T \boldsymbol{\psi}_e \cdot \boldsymbol{\psi}_{e'} \\
&\leq \sum_T \sum_{e \in \partial T} \sum_{e' \in \partial T} |\sigma_e(\mathbf{u})| |\sigma_{e'}(\mathbf{u})| \|\boldsymbol{\psi}_e\|_{0,\alpha,T} \|\boldsymbol{\psi}_{e'}\|_{0,\alpha,T} \\
&\leq \frac{1}{2} \sum_T \sum_{e \in \partial T} \sum_{e' \in \partial T} ([\sigma_e(\mathbf{u})]^2 \|\boldsymbol{\psi}_e\|_{0,\alpha,T}^2 + [\sigma_{e'}(\mathbf{u})]^2 \|\boldsymbol{\psi}_{e'}\|_{0,\alpha,T}^2) \\
&= (d+1) \sum_T \sum_{e \in \partial T} [\sigma_e(\mathbf{u})]^2 \|\boldsymbol{\psi}_e\|_{0,\alpha,T}^2.
\end{aligned}$$

In the last step we have used $\sum_{e \in \partial T} 1 = (d+1)$. Switching the order of summation in the right side of the inequality above then gives

$$\begin{aligned}
\|\mathbf{u}\|_{0,\alpha}^2 &\leq (d+1) \sum_{e \in \mathcal{E}_h} \left(\|\boldsymbol{\psi}_e\|_{0,\alpha,T_e^+}^2 + \|\boldsymbol{\psi}_e\|_{0,\alpha,T_e^-}^2 \right) [\sigma_e(\mathbf{u})]^2 \\
&= (d+1) \sum_{e \in \mathcal{E}_h} \hat{\alpha}_e [\sigma_e(\mathbf{u})]^2 \|\boldsymbol{\psi}_e\|^2 = (d+1) \|\mathbf{u}\|_{*,\hat{\alpha}}^2.
\end{aligned}
\tag{A.8}$$

To prove the equivalence in (i) for $\hat{\alpha}_e = 1$, $e \in \mathcal{E}_h$, we observe that for $T \in \mathcal{T}_h$ we have the following equivalence relation with constants only depending on the geometry of T (bounded for shape regular triangulation):

$$\sum_{e \in \partial T} \sum_{e' \in \partial T} \sigma_e(\mathbf{u})\sigma_{e'}(\mathbf{u}) \int_T \boldsymbol{\psi}_e \boldsymbol{\psi}_{e'} \approx \sum_{e \in \partial T} [\sigma_e(\mathbf{u})]^2 \|\boldsymbol{\psi}_e\|^2.
\tag{A.9}$$

The equivalence (A.9) is just spectral equivalence between the element mass matrix $\{(\boldsymbol{\psi}_e, \boldsymbol{\psi}_{e'})\}_{e,e' \in \partial T}$ and its diagonal $\{\|\boldsymbol{\psi}_e\|^2\}_{e \in \partial T}$ which is easy to establish, for example, by using the explicit form of the basis functions given in (A.2) and (A.3). This completes the proof of (i).

Items (ii) and (iii) directly follow from the definitions and the inequality (2.7) which implies that $\|\alpha\|_{\ell^2} \leq 1$. \square

An immediate corollary from Proposition A.1 and Lemma A.1 is the following Poincaré inequality.

Corollary A.1. *If $\omega_e = 1$ for all $e \in \mathcal{E}_h$ we have*

$$\|\chi\|^2 \leq C_P \|\nabla_h \chi\|_{*,1}^2,
\tag{A.10}$$

with a constant C_P independent of h .

Proof. To prove this Poincaré inequality we recall a classical result on the solvability of the mixed discretizations of the Laplace equation. It is well known (see, for example, [4, (7.1.28) and Proposition 5.4.3]; also [3]), that the following estimate holds with $\tilde{\gamma} > 0$ independent of h for all $q \in W_h$:

$$\sup_{\mathbf{v} \in \mathbf{V}_h} \frac{(q, \text{div } \mathbf{v})}{\|\mathbf{v}\|_{\Lambda_1}} \geq \tilde{\gamma} \|q\|.
\tag{A.11}$$

Since by Lemma A.1(i) the norms $\|\cdot\|$ and $\|\cdot\|_{*,1}$ are equivalent norms on \mathbf{V}_h , for any $\chi \in W_h$:

$$\begin{aligned} \|\nabla_h \chi\|_{*,1} &= \sup_{\mathbf{v} \in \mathbf{V}_h} \frac{(\nabla_h \chi, \mathbf{v})_{*,1}}{\|\mathbf{v}\|_{*,1}} = \sup_{\mathbf{v} \in \mathbf{V}_h} \frac{(\chi, \operatorname{div} \mathbf{v})}{\|\mathbf{v}\|_{*,1}} \\ &\gtrsim \sup_{\mathbf{v} \in \mathbf{V}_h} \frac{(\chi, \operatorname{div} \mathbf{v})}{\|\mathbf{v}\|} \geq \sup_{\mathbf{v} \in \mathbf{V}_h} \frac{(\chi, \operatorname{div} \mathbf{v})}{\|\mathbf{v}\|_{\Lambda_1}} \geq \tilde{\gamma} \|\chi\|. \end{aligned}$$

Therefore, (A.10) holds with $C_P = \tilde{\gamma}^{-2}$. \square

Remark A.1. Clearly, for a scalar coefficient $K(x)$ the edge weights $\hat{\kappa}_e$ are weighted harmonic averages of the values of the coefficient on the two elements sharing the face e . On a uniform mesh, where $\|\psi_e\|_{0,\alpha,T_e^\pm}^2 / \|\psi_e\|^2 = |\alpha_{T_e^\pm}|/2$ we have that

$$\hat{\kappa}_e = \frac{2K_{+,e}K_{-,e}}{K_{+,e} + K_{-,e}}$$

On a non-uniform mesh or for tensor coefficient $K(x)$ the average is more complicated and involves weights depending on geometrical quantities describing pairs of neighboring elements.

Consider now $q \in W_h$ and let $\varphi \in W_h$ be the solution of the variational problem

$$(A.12) \quad (D_{\hat{\kappa}} \nabla_h \varphi, \nabla_h \chi)_{*,1} = (q, \chi), \quad \text{for all } \chi \in W_h.$$

In accordance with Proposition A.1(ii) the solution to the variational problem (A.12) φ exists and is unique. We further set

$$(A.13) \quad \mathbf{w} = D_{\hat{\kappa}} \nabla_h \varphi$$

and by the definition of ∇_h we have $-(\operatorname{div} D_{\hat{\kappa}} \nabla_h \varphi, \chi)_{*,1} = (q, \chi)$ for all $\chi \in W_h$, which implies that

$$(A.14) \quad \operatorname{div} D_{\hat{\kappa}} \nabla_h \varphi = -q.$$

Next, we prove an a priori estimate needed for the proof of a contrast independent inf-sup condition.

Lemma A.2. Let $\varphi \in W_h$ be the solution of (A.12) and let $\mathbf{w} \in \mathbf{V}_h$ be defined as in (A.13), namely, $\mathbf{w} = D_{\hat{\kappa}} \nabla_h \varphi$. Then the following a priori estimate holds

$$(A.15) \quad \|\mathbf{w}\|_{*,\hat{\alpha}}^2 \leq 2C_P \|q\|^2.$$

Proof. The proof follows from Proposition A.1, Lemma A.1 and some simple equalities. We have

$$\begin{aligned} \|\mathbf{w}\|_{*,\hat{\alpha}}^2 &= (D_{\hat{\alpha}} \mathbf{w}, \mathbf{w})_{*,1} && [\text{by Proposition A.1(i)}] \\ &= (D_{\hat{\alpha}} D_{\hat{\kappa}} \nabla_h \varphi, \mathbf{w})_{*,1} && [\text{by the definition of } \mathbf{w}] \\ &= (\nabla_h \varphi, \mathbf{w})_{*,1} && \text{by [Lemma A.1(ii)]} \\ &= -(\varphi, \operatorname{div} \mathbf{w}) = (\varphi, q) \leq \|\varphi\| \|q\|. && [\text{by (A.14)}] \end{aligned}$$

We now use the Poincaré inequality to estimate $\|\varphi\|$:

$$\begin{aligned} \|\varphi\|^2 &\leq C_P (\nabla_h \varphi, \nabla_h \varphi)_{*,1} && [\text{by (A.10)}] \\ &\leq 2C_P (D_{\hat{\kappa}} \nabla_h \varphi, \nabla_h \varphi)_{*,1} && [\text{by Lemma A.1(iii)}] \\ &= 2C_P (D_{\hat{\kappa}} \nabla_h \varphi, D_{\hat{\alpha}} D_{\hat{\kappa}} \nabla_h \varphi)_{*,1}, && [\text{by Lemma A.1(ii)}] \\ &= 2C_P \|\mathbf{w}\|_{*,\hat{\alpha}}^2 && [\text{by the definition of } \mathbf{w}] \end{aligned}$$

Note that we have used the inequality $\hat{\kappa}_e \geq \frac{1}{2}$ for all $e \in \mathcal{E}_h$. \square

After all the preparatory work, we are ready to prove the discrete inf-sup condition.

Theorem A.2. *The following inequality holds with constant $\gamma > 0$ independent of the contrast κ :*

$$(A.16) \quad \inf_{q \in W_h} \sup_{\mathbf{v} \in \mathbf{V}_h} \frac{(q, \text{div } \mathbf{v})}{\|\mathbf{v}\|_{\Lambda_\alpha} \|q\|} \geq \gamma.$$

Proof. For all $q \in W_h$ and with \mathbf{w} defined as in (A.13) we have

$$\begin{aligned} \sup_{\mathbf{v} \in \mathbf{V}_h} \frac{(q, \text{div } \mathbf{v})}{\|\mathbf{v}\|_{\Lambda_\alpha}} &\geq \|q\|^2 / (\|\mathbf{w}\|_{0,\alpha}^2 + \|\text{div } \mathbf{w}\|^2)^{\frac{1}{2}} && [\text{by the definition of sup}] \\ &\geq \|q\|^2 / \left((d+1) \|\mathbf{w}\|_{*,\hat{\alpha}}^2 + \|\text{div } \mathbf{w}\|^2 \right)^{\frac{1}{2}} && [\text{by Lemma A.1(i)}] \\ &= \|q\|^2 / \left((d+1) \|\mathbf{w}\|_{*,\hat{\alpha}}^2 + \|q\|^2 \right)^{\frac{1}{2}} && [\text{by (A.14)}] \\ &\geq \|q\| / \sqrt{2(d+1)C_P + 1}, && [\text{by Lemma A.2}] \end{aligned}$$

which completes the proof. \square

The standard theory of mixed finite element methods then immediately implies the following approximation result

Theorem A.3. *Let $(\mathbf{u}, p) \in \mathbf{H}_N(\text{div}) \times L_2$ be the solution of the mixed problem (2.10) and $(\mathbf{u}_h, p_h) \in \mathbf{V}_h \times W_h$ be the solution of the discrete problem (3.3). Then the following estimate holds*

$$(A.17) \quad \|\mathbf{u} - \mathbf{u}_h\|_{\Lambda_\alpha} + \|p - p_h\| \leq C \left(\inf_{\mathbf{v} \in \mathbf{V}_h} \|\mathbf{u} - \mathbf{v}\|_{\Lambda_\alpha} + \inf_{q \in W_h} \|p - q\| \right),$$

where the constant C depend on the shape regularity of the mesh, the Poincaré constant C_P , and the spatial dimension d , but is independent of the variations in $K(x)$.

ACKNOWLEDGMENTS

This work has been partially supported by the Bulgarian NSF Grant DCVP 02/1, FP7 Grant AComIn, and the Austrian NSF Grant P22989. R. Lazarov has been supported in parts by US NSF Grant DMS-1016525, by Award No. KUS-C1-016-04, made by KAUST. L. Zikatanov has been supported in part by US NSF Grants DMS-1217142 and DMS-1016525.

REFERENCES

- [1] D. Arnold, R. Falk, and R. Winther. Preconditioning in $\mathbf{H}(\text{div})$ and applications. *Mathematics of Computation*, 66:957–984, 1997.
- [2] D. Arnold, R. Falk, and R. Winther. Multigrid in $\mathbf{H}(\text{div})$ and $\mathbf{H}(\text{curl})$. *Numerische Mathematik*, 85(2):197–217, 2000.
- [3] D. N. Arnold. Differential complexes and numerical stability. In *Proceedings of the International Congress of Mathematicians, Vol. I (Beijing, 2002)*, pages 137–157, Beijing, 2002. Higher Ed. Press.
- [4] D. Boffi, F. Brezzi, and M. Fortin. *Mixed finite element methods and applications*, volume 44 of *Springer Series in Computational Mathematics*. Springer, Heidelberg, 2013.
- [5] F. Brezzi and M. Fortin. *Mixed and hybrid finite element methods*. Springer, New York, 1991.
- [6] A. Ern and J.-L. Guermond. *Theory and Practice of Finite Elements*, volume 159. Springer, 2004.
- [7] S. P. E. International. SPE10 comparative solution project: general information and description of model 2, 2000. <http://www.spe.org/web/csp/#datasets>.
- [8] J. Kraus. Additive Schur complement approximation and application to multilevel preconditioning. *SIAM Journal on Scientific Computing*, 34(6):A2872–A2895, 2012.
- [9] J. Kraus, M. Lymbery, and S. Margenov. Auxiliary space method based on additive Schur complement approximation. *Numerical Linear Algebra with Applications*, NLA-13-0127. (submitted Oct. 2013).
- [10] J. Kraus and S. Margenov. *Robust Algebraic Multilevel Methods and Algorithms*. De Gruyter Incorporated, Walter, Berlin-New York, 2009.
- [11] J. Kraus, P. Vassilevski, and L. Zikatanov. Polynomial of best uniform approximation to $1/x$ and smoothing for two-level methods. *Comput. Meth. Appl. Math.*, 12:448–468, 2012.

- [12] A. Matsokin and S. Nepomnyashchikh. The Schwarz alternation method in a subspace. *Izv. Vyssh. Uchebn. Zaved. Mat.*, (10):61–66, 85, 1985.
- [13] S. Nepomnyashchikh. Mesh theorems on traces, normalizations of function traces and their inversion. *Soviet J. Numer. Anal. Math. Modelling*, 6(3):223–242, 1991.
- [14] S. Nepomnyashchikh. Fictitious space method on unstructured meshes. *East-West J. Numer. Math*, 3(1):71–79, 1995.
- [15] A. Pehlivanov, G. Carey, and R. Lazarov. Least-squares mixed finite elements for second-order elliptic problems. *SIAM Journal on Numerical Analysis*, 31(5):1368–1377, 1994.
- [16] P. Vassilevski. *Multilevel block factorization preconditioners: Matrix-based Analysis and Algorithms for Solving Finite Element Equations*. Springer, New York, 2008. Matrix-based analysis and algorithms for solving finite element equations.
- [17] P. S. Vassilevski and R. D. Lazarov. Preconditioning mixed finite element saddle-point elliptic problems. *Numerical Linear Algebra with Applications*, 3(1):1–20, 1996.
- [18] J. Xu. The auxiliary space method and optimal multigrid preconditioning techniques for unstructured grids. *Computing*, 56:215–235, 1996.
- [19] J. Xu and L. Zikatanov. Some observations on Babuska and Brezzi theories. *Numerische Mathematik*, 94(1):195–202, 2003.

THEA-LEYMANN-STR. 9 45141 ESSEN, GERMANY
E-mail address: johannes.kraus@uni-due.de

DEPARTMENT OF MATHEMATICS, TEXAS A & M UNIVERSITY, COLLEGE STATION, TX 77843, USA AND INSTITUTE OF MATHEMATICS AND INFORMATICS, BULGARIAN ACADEMY OF SCIENCES, ACAD. G. BONCHEV ST., BL. 8, 1113 - SOFIA, BULGARIA
E-mail address: lazarov@math.tamu.edu

INSTITUTE OF INFORMATION AND COMMUNICATION TECHNOLOGIES, BULGARIAN ACADEMY OF SCIENCES, ACAD. G. BONCHEV ST., BLOCK 2, 1113 - SOFIA, BULGARIA
E-mail address: mariq@parallel.bas.bg

INSTITUTE OF INFORMATION AND COMMUNICATION TECHNOLOGIES, BULGARIAN ACADEMY OF SCIENCES, ACAD. G. BONCHEV ST., BLOCK 2, 1113 - SOFIA, BULGARIA
E-mail address: margenov@parallel.bas.bg

DEPARTMENT OF MATHEMATICS, THE PENNSYLVANIA STATE UNIVERSITY, UNIVERSITY PARK, PA 16802, USA
E-mail address: ludmil@psu.edu